Wideband Direction-of-Arrival (DOA) Estimation Methods for Unattended Acoustic Sensors

Nicholas Roseveare

Department of Electrical and Computer Engineering
Colorado State University

Thesis Defense, September 28, 2007

Outline of Presentation

Background on DOA Estimation using UGS

Unattended ground sensors (UGS) have application in battlefield surveillance and situation awareness:

- They are rugged, reliable, and can be left in the field for a long time after deployment
- They can be used to capture acoustic signatures of a variety of sources in different types of terrain (MOUT, etc.)
- The acoustic information may then be used to spatially locate and track sources such as ground vehicles, airborne targets, or even personnel

Generally, high performance DOA estimation can separate multiple closely spaced sources. Complications to this arise in acoustic arrays due to:

- Variability and nonstationarity of source acoustic signatures
- Signal attenuation and fading effects as a function of range and Doppler
- Coherence loss due to environmental conditions and wind effects
- Near-field, multipath, or other non-plane wave effects

Review of Literature

Direction-of-Arrival (DOA) estimation

- Wideband DOA estimation and tracking with acoustic arrays
  [Pham] Benchmark of wideband DOA estimation algorithms[1]
  [Azimi] Localization of multiple wideband sources and the use of distributed arrays to combat sensor location and non-uniform fading error[2, 3]
  [Damarla],[Hohil] Tracking, counting, and classifying vehicles[4, 5]
- Narrowband DOA estimation algorithms with application to acoustic arrays
  [Capon] Minimum Power Distortionless Response (MPDR)[6]
  [Schmidt] MUltiple SIgnal Classification (MUSIC) method[7]
  [Viberg] Weighted Subspace Fitting (WSF) method[8]

Review of Literature

- Wideband frequency combining methods
  [Krolik] Coherent focusing with Steered Covariance Matrices[9, 10]
  [Pham],[Azimi] Wideband incoherent averaging methods[11, 2]
  [Kaveh],[Di Claudio] Coherent MUSIC and WSF[12, 13]
- Non-idealized array source models for DOA estimation
  [Swindlehurst] Models for array geometry and calibration errors[14]
  [Asztély] Multipath model for local scattering[15, 16]
  [Valaee] Models for spatially coherent or incoherent sources[17]
  [Meng],[Scharf] Array source model for partial incoherence[18, 19, 20]

Objectives of this Research

- To benchmark and illustrate deficiencies in existing wideband DOA estimation algorithms
- To develop a better understanding of non-ideal array signal models
- This understanding will help appropriately modify the computationally simple Capon to make it robust to the errors in our acoustic data sets
- To benchmark and show the performance improvements of the developed algorithms

Outline

Wideband Signal Model

Consider d far-field sources observed by L sensors in an arbitrary noise wavefield for frequency bin f_j and sample k

$$\mathbf{x}(f_j,k) = \mathbf{A}(f_j,\phi)\mathbf{s}(f_j,k) + \mathbf{n}(f_j,k) = \sum_{i=1}^{d} \mathbf{a}(f_j,\phi_i)s_i(f_j,k) + \mathbf{n}(f_j,k) \quad (1)$$

$\mathbf{A}(f_j,\phi) = [\mathbf{a}(f_j,\phi_1),\ldots,\mathbf{a}(f_j,\phi_d)]$	array manifold of steering vectors
$\mathbf{s}(f_j,k) = [s_1(f,k),\ldots,s_d(f,k)]^T$	vector of sources
$\phi = [\phi_1,\ldots,\phi_d]$	vector of source directions
$\mathbf{n}(f_j,k)$	noise vector

The sample covariance matrix for frequency f_j is given as

$$\mathbf{R_{xx}}(f_j) = \sum_{k=1}^{K} \mathbf{x}(f_j,k)\mathbf{x}^H(f_j,k) = \mathbf{A}(f_j,\theta)\mathbf{R_s}(f_j)\mathbf{A}^H(f_j,\theta) + \mathbf{R_n}(f_j)$$

Basic DOA Estimation: Beamforming

- The most basic DOA estimation method is the beamformer which is given by the inner product of the array output vector and a weight vector as

$$y(f_j, k, \theta) = \mathbf{w}^H(f_j, \theta)\mathbf{x}(f_j, k), \tag{2}$$

  where the weight vector $\mathbf{w}(f_j, \theta)$ steers the beam response of the array to observation angle, θ.
- The quadratic power spectrum becomes

$$p(f_j, \theta) = \mathbf{w}^H(f_j, \theta)\mathbf{R}_{\mathbf{xx}}(f_j)\mathbf{w}(f_j, \theta), \tag{3}$$

  from which the peaks are used as DOA estimates.

Capon Beamforming

Minimizes the overall received power while requiring the signal of interest (SOI) to be received at unit power, i.e.

$$\min_{\mathbf{w}(f_j,\theta)} \mathbf{w}^H(f_j,\theta)\mathbf{R}_{\mathbf{xx}}\mathbf{w}(f_j,\theta) \;\; s.t. \; \mathbf{w}^H(f_j,\theta)\mathbf{a}(f_,\theta) = 1 \tag{4}$$

This results in the optimal beamformer weights

$$\mathbf{w}^*(f_j,\theta) = \frac{\mathbf{R}_{\mathbf{xx}}^{-1}(f_j)\mathbf{a}(f_j,\theta)}{\mathbf{a}^H(f_j,\theta)\mathbf{R}_{\mathbf{xx}}^{-1}(f_j)\mathbf{a}(f_j,\theta)}, \tag{5}$$

this beamformer yields the power spectrum

$$p_{Capon}(f_j,\theta) = \frac{1}{\mathbf{a}^H(f_j,\theta)\mathbf{R}_{\mathbf{xx}}^{-1}(f_j)\mathbf{a}(f_j,\theta)}. \tag{6}$$

incoherent averaging across frequency using the geometric mean is

$$P_G(\theta) = \prod_{j=1}^{J} p_{Capon}(f_j,\theta) = \prod_{j=1}^{J} \frac{1}{\mathbf{a}^H(f_j,\theta)\mathbf{R}_{\mathbf{xx}}^{-1}(f_j)\mathbf{a}(f_j,\theta)}.$$

Review MUSIC, WSF, and STCM

	Idea	Drawbacks
MUSIC	Exploits orthogonality between signal and noise subspaces, DOA estimate is min distance between steering vector and noise eigenvectors	Sensitive to choice of noise subspace and requires SVD
WSF	Fits data to a search array manifold matrix in least-squares sense, DOA estimates found from minimum of error between fitted and actual array response	Requires SVD and an intense multi-dimensional search over sets of angles
STCM	Uses unitary transforms to focuses the frequency spectra from multiple narrowband bins; applied in tandem with a narrowband algorithm	Focusing reduces the resolution capabilities of whichever algorithm it is used with

Results on Baseline and Distributed Array Data Sets

The baseline array data:

- Textron® five-element wagon-wheel ADAS type array
- A variety of military vehicle types provided acoustic sources
- Samples were collected at $1024Hz$ for the uncalibrated time series
- Phase/gain calibration for $50 - 250Hz$ and 50% overlap sliding Hamming window produced 2048 samples per observation period for the calibrated data

The distributed array data:

- Fifteen wireless Crossbow Telos® sensor nodes
- Two types of mid-sized moving trucks were the acoustic sources
- Samples were collected at $1024Hz$; only 876 samples per observation period
- No calibration; additional error due to sensor position uncertainty (up to $.2m$) due to GPS measurement error

DOA Estimation Results - Baseline Run 1

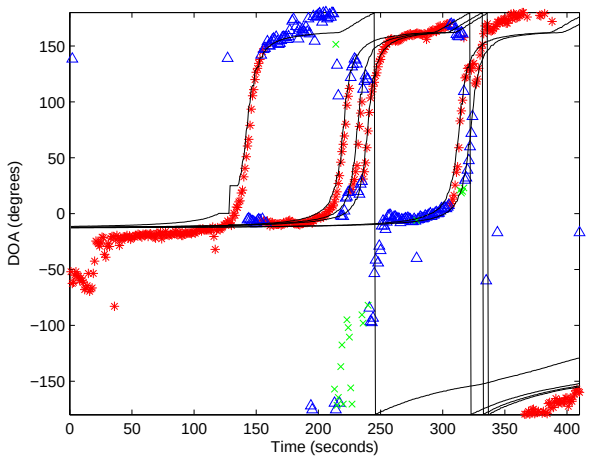

Arithmetic Capon

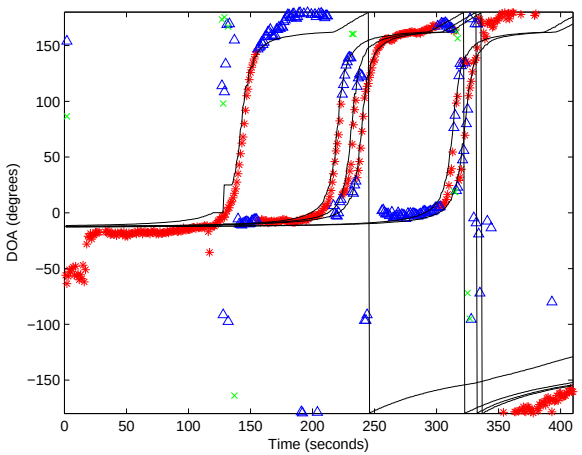

Geometric Capon

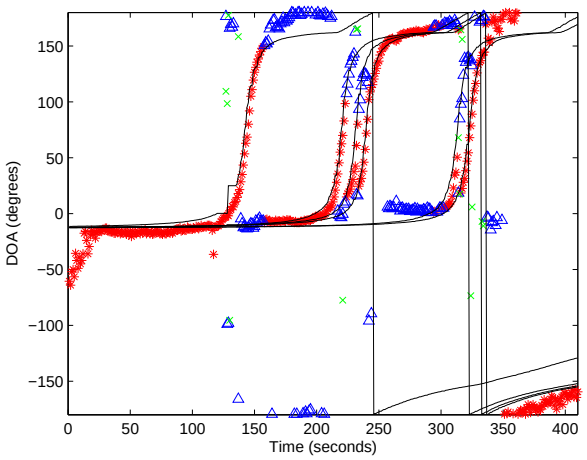

Harmonic Capon

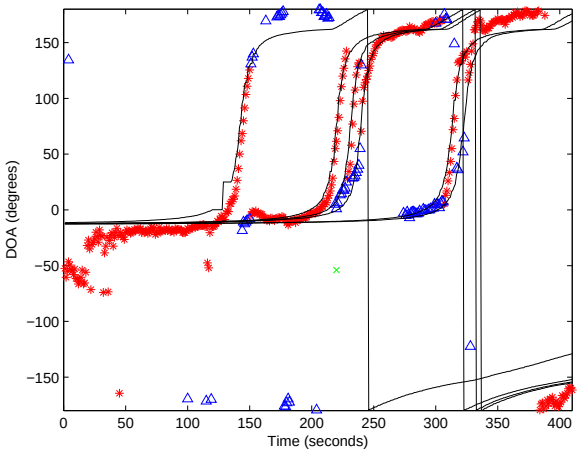

STCM

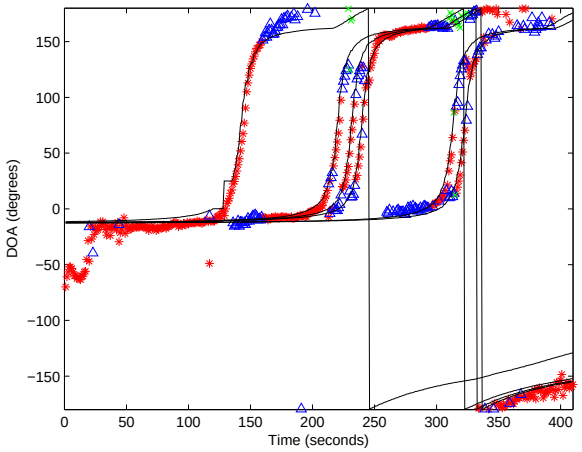

Geometric MUSIC

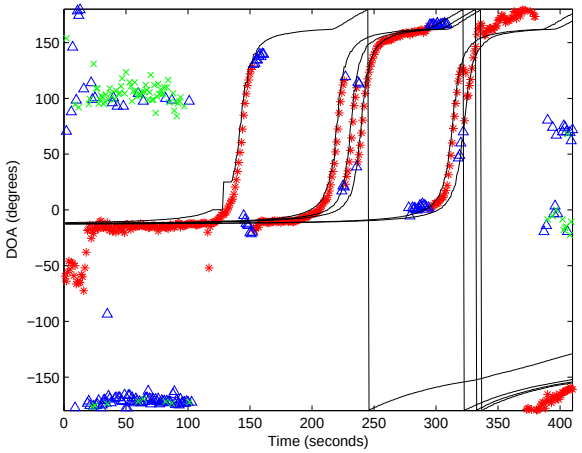

WSF

The markers '$*$', '$\triangle$', and '$\times$' or '$\times$', correspond to the DOAs obtained from the first, second, and third peaks of the spectrum.

DOA Estimation Results - Baseline Run 4

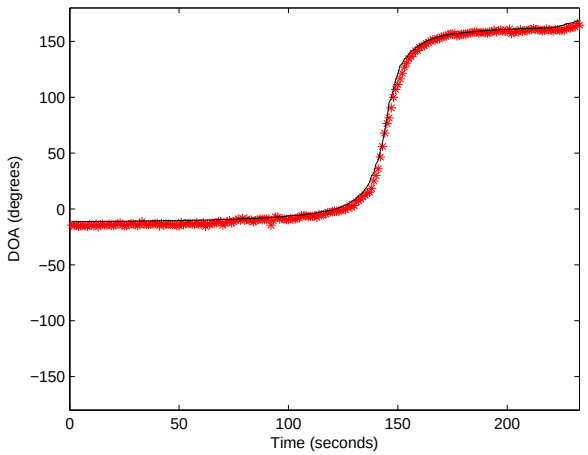

Arithmetic Capon

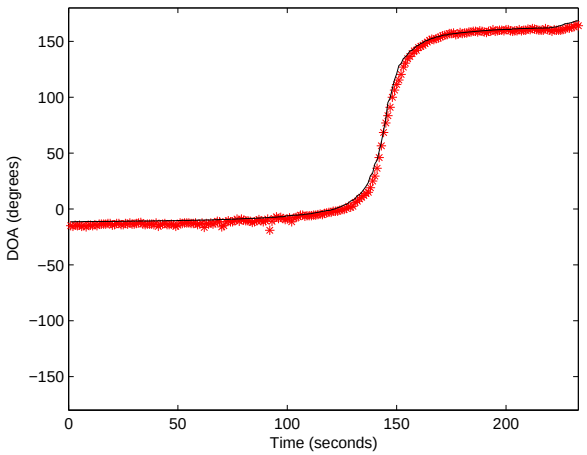

Geometric Capon

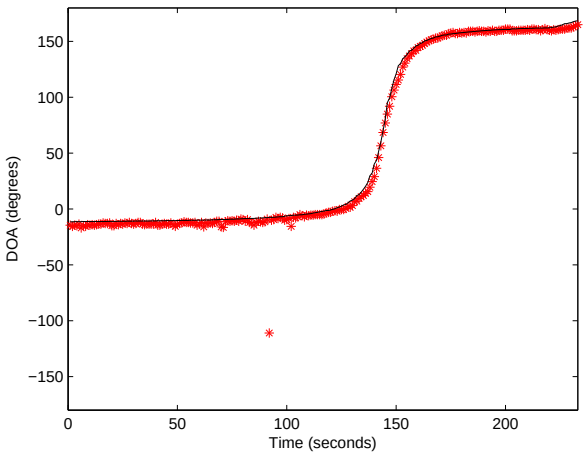

Harmonic Capon

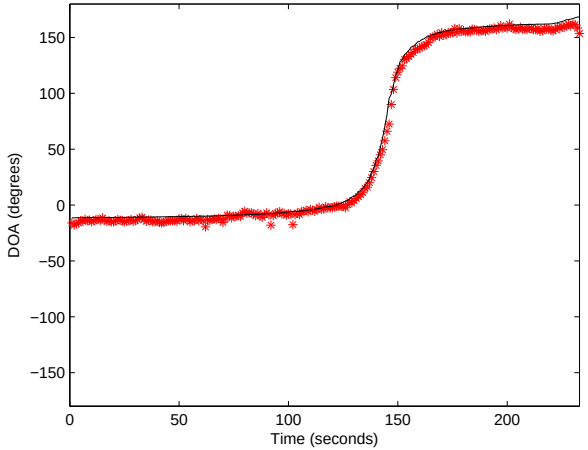

STCM

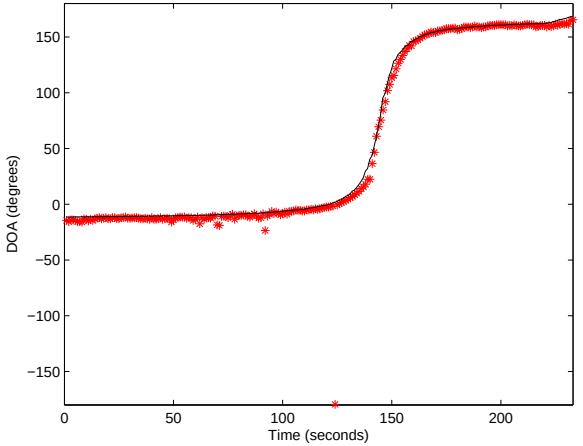

Geometric MUSIC

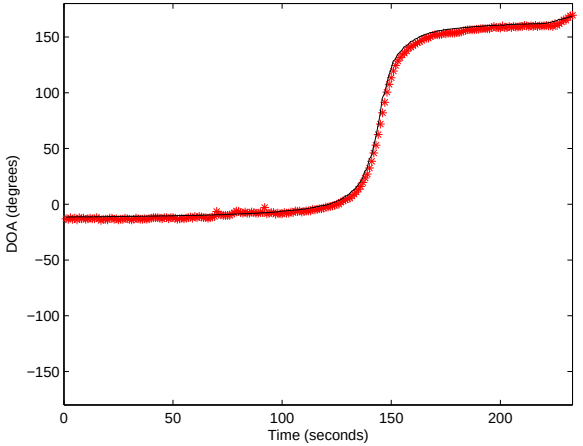

WSF

Error Statistics for Run 4

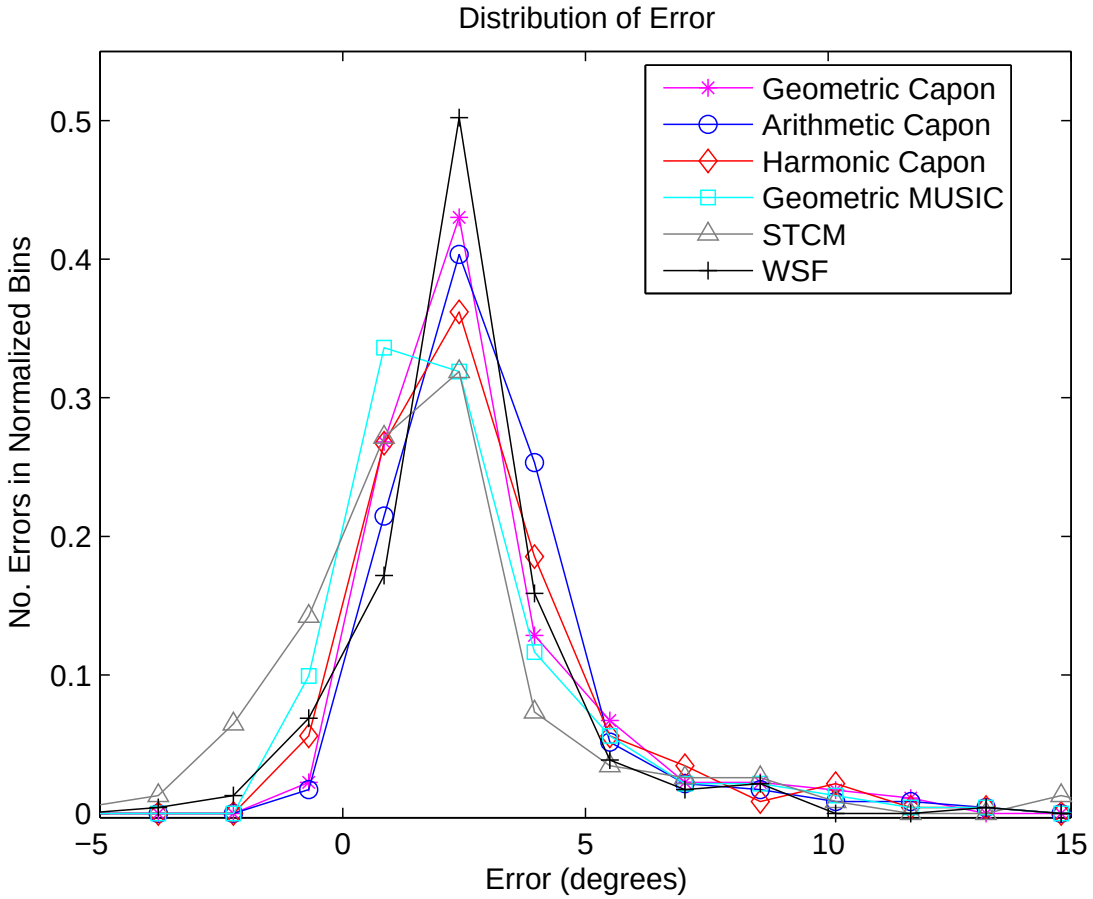

	Geo. Capon	Ari. Capon	STCM	Har. Capon	Geo. MUSIC	WSF
μ_e	2.8619°	2.9778°	3.3340°	2.7903°	* 2.5633°	2.6842°
σ_e^2	5.0469	4.2967	8.1961	4.9874	6.8435	* 3.0665

DOA Estimation Results - Distributed Run 2

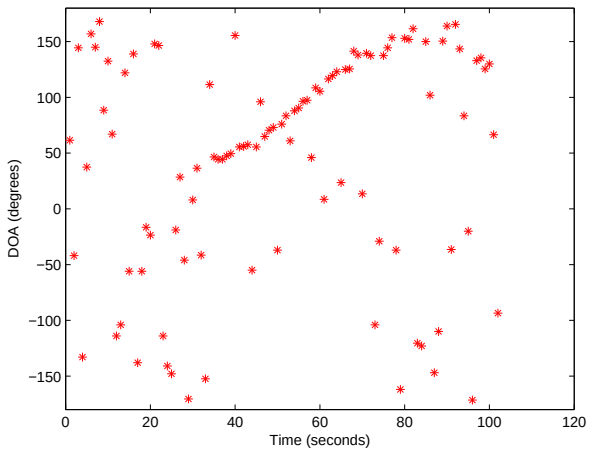

Arithmetic Capon

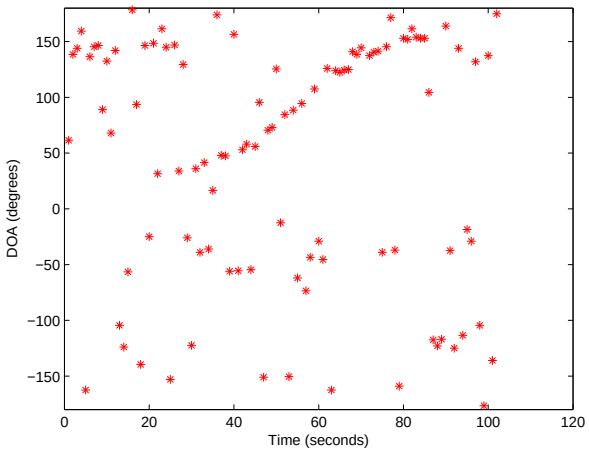

Geometric Capon

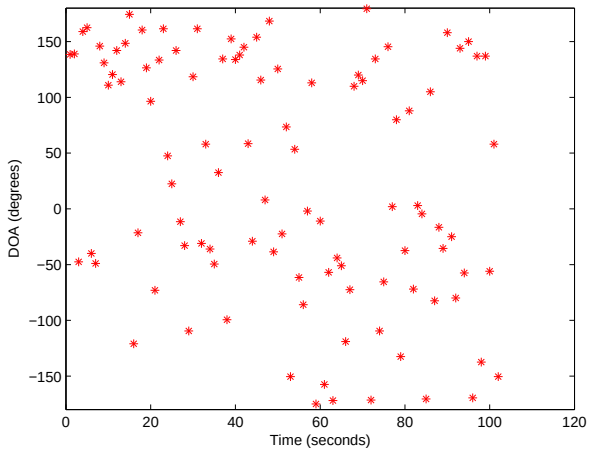

Harmonic Capon

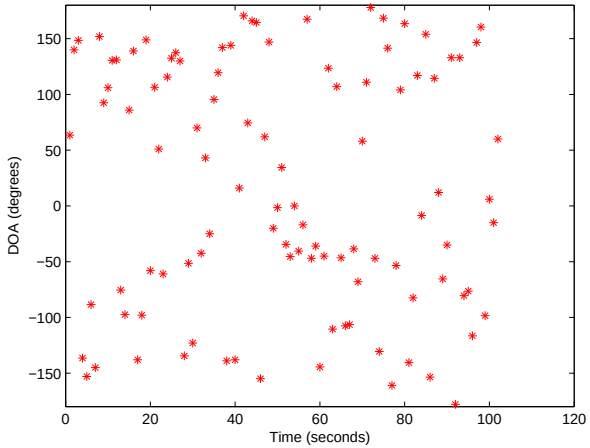

STCM

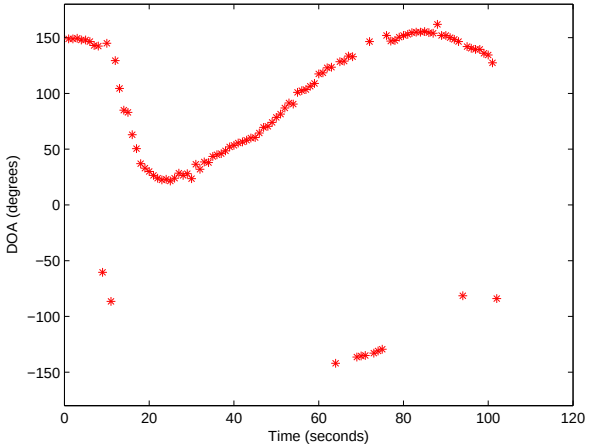

Geometric MUSIC

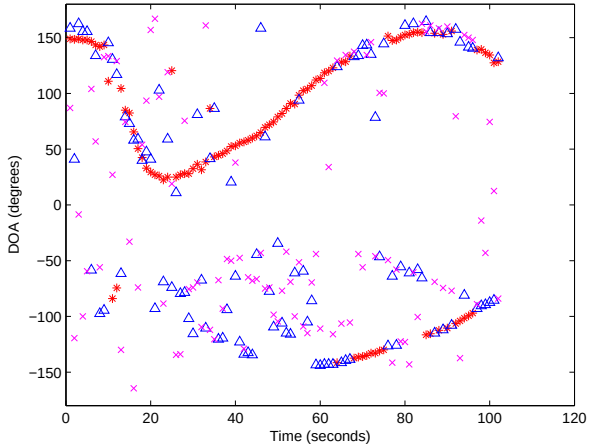

WSF

DOA Estimation Results - Distributed Run 2

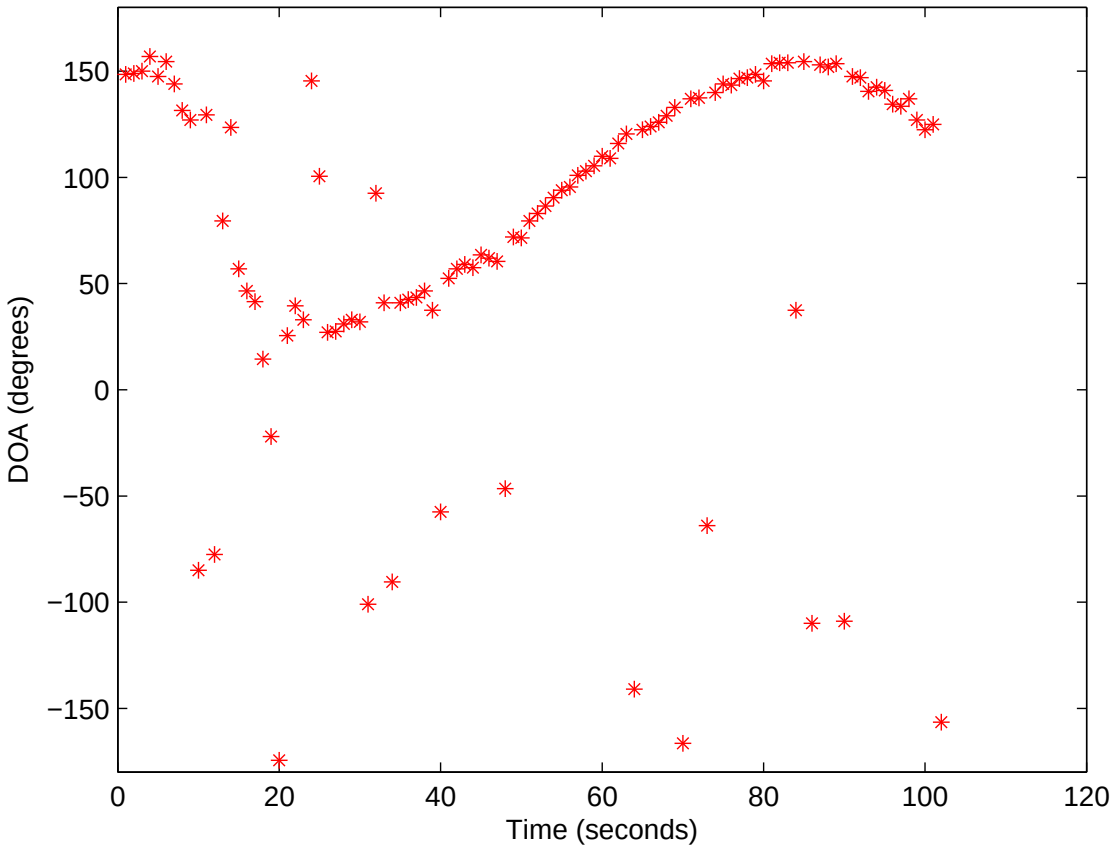

DOA Estimates using geometric Capon for Run 2 with the failed node (node 2) removed.

Outline

The Need for a General Error Model

The reviewed models have been reduced to an understanding of the type of error coherence the source has and how this affects the covariance matrix.

This is important because

- It is useful to have a general model for different errors which you can tailor to the type error present in a particular scenario
- The basis for developing a particular robust algorithm is expressly dependent on the coherence of the error or mismatch assumed present in the data
    - The error coherence distinguishes the rank of the source in the covariance matrix, and therefore determines how to develop an algorithm to match to this source.

Error Models in terms of Source Coherence

Coherence types

- Complete spatial coherence. This response models sources which are spatially coherent and temporally persistent within the observation period.
  - Sensor position error, phase/gain or other array miscalibration
  - Near-field effects and local scattering multipath effects
- Complete spatial incoherence. For this case there is no spatial coherence between source samples during the observation period.
  - Uncorrelated reflections of a source off tropospheric scatterers (radiowave source)
- Partial spatial incoherence. The spatial coherence of the source in this scenario persists infrequently throughout the observation period.
  - Multipath for non-local scattering
  - When the array geometry is flexible and alters within the observation period

Array and Calibration Error Model

- This type of error includes: Sensor position error, array miscalibration, quantization errors, gain/phase errors, other errors without structure.
- The array signal model for this type of error can be expressed as the nominal response, $\mathbf{A}(f_j, \theta)$, plus an error matrix, $\tilde{\mathbf{A}}(f_j, \theta)$. The perturbed sample covariance can be written as

$$\tilde{\mathbf{R}}_{\mathbf{xx}}(f_j) = (\mathbf{A}(f_j, \theta) + \tilde{\mathbf{A}}(f_j, \theta))\mathbf{R}_{\mathbf{s}}(f_j)(\mathbf{A}(f_j, \theta) + \tilde{\mathbf{A}}(f_j, \theta))^H + \mathbf{R}_{\mathbf{n}}(f_j). \quad (7)$$

- The structure of the array manifold has changed, but the perturbed signal covariance is still rank-one.

Multipath Model

This multipath model considers local scattering. The array response is the sum of multiple coherent planewaves arriving at nearby angles. Thus the multipath spatial response for the ith source is

$$\mathbf{v}_i(f_j, \phi_i) = \sum_{k=1}^{N_i} \alpha_{ik}(f_j)\mathbf{a}(f_j, \phi_i + \tilde{\phi}_{ik}). \tag{8}$$

The local scattering enables a first order derivative approximation and results in the following spatial covariance

$$\mathbf{R_{xx}}(f_j) = [\mathbf{A}(f_j, \phi) + \mathbf{D}(f_j, \phi)]\mathbf{\Gamma}(f_j)\mathbf{R_s}(f_j)\mathbf{\Gamma}^H(f_j)[\mathbf{A}(f_j, \phi) + \mathbf{D}(f_j, \phi)] + \mathbf{R_n}(f_j). \tag{9}$$

where $\mathbf{\Gamma}(f_j)$ is a diagonal fading matrix and $\mathbf{D}(f_j, \phi)$ is the first derivative of the array manifold (by vector). As is evident, this is still a rank-one matrix. This would be similar for near-field effects.

Model for Coherent and Incoherent Sources

Consider the noise-free covariance matrix for the ith source (uncorrelated from other sources)

$$\mathbf{R}_i(f_j, \boldsymbol{\psi}) = \int_{\phi \in \Phi} \int_{\phi' \in \Phi} \mathbf{a}(f_j, \phi) p_i(f_j, \phi, \phi'; \boldsymbol{\psi}_i) \mathbf{a}^H(f_j, \phi') d\phi d\phi' \tag{10}$$

where, for the ith source,

- $\boldsymbol{\psi}_i$ spreading parameter vector
- $p_i(f_j, \phi, \phi'; \boldsymbol{\psi}_i) = E[s_i(f_j, \phi; \boldsymbol{\psi}_i) s_i^*(f_j, \phi'; \boldsymbol{\psi}_i)]$ is the *angular auto-correlation*

The coherent source signal density can be written as

$$s_i(f_j, \phi; \boldsymbol{\psi}_i) = \gamma_i(f_j) g(f_j, \phi; \boldsymbol{\psi}_i) \tag{11}$$

which results in the angular auto correlation function (ACF)

$$p(f_j, \phi, \phi'; \boldsymbol{\psi}) = \eta(f_j,) g(f_j, \phi; \boldsymbol{\psi}) g^*(f_j, \phi'; \boldsymbol{\psi}). \tag{12}$$

The incoherent source angular ACF is

$$p(f_j, \phi, \phi'; \boldsymbol{\psi}) = p(f_j, \phi; \boldsymbol{\psi}) \delta(\phi - \phi'). \tag{13}$$

Conclusions on Source Error Coherence

Cohrence types

- Complete spatial coherence. This response models sources which are spatially coherent that persist temporally within the observation period.
  - Rank one source covariance of unknown structure. This corresponds to the type of error coherence in the data sets of this study.
- Complete spatial incoherence. For this case there is no coherence between source samples during the observation period.
  - Full rank source covariance.
- Partial spatial incoherence. The coherence in this scenario persists infrequently throughout the observation period.
  - Multi-rank source covariance, but typically not full rank.

Outline

Review of Wideband Robust Capon Algorithm

- The robust Capon is designed to be robust against rank-one errors in the steering vector, i.e. sensor position error and near-field effects.
- It belongs to the class of diagonal loading approaches for robust estimation and is introduced by Li and Stoica[21].
- It operates based on an ellipsoidal uncertainty constraint for the steering vector and is formulated as

$$\min_{\mathbf{a}} \ \mathbf{a}^H(f_j,\theta)\mathbf{R}_{\mathbf{xx}}^{-1}(f_j)\mathbf{a}(f_j,\theta) \quad s.t. \quad \| \mathbf{a}(f_j,\theta) - \bar{\mathbf{a}}(f_j,\theta) \|^2 \leq \epsilon. \tag{14}$$

The optimal beamformer weight vector is

$$\mathbf{w}(f_j,\theta) = \bar{\mathbf{a}}(f_j,\theta) - \mathbf{U}(f_j)(I + \lambda(f_j)\mathbf{\Sigma}(f_j))^{-1}\mathbf{U}^H(f_j)\bar{\mathbf{a}}(f_j,\theta). \tag{15}$$

The wideband robust Capon power spectrum becomes

$$P_{G_{Robust}}(\theta) = \prod_{j=1}^{J} \frac{1}{\bar{\mathbf{a}}^H(f_j,\theta)\mathbf{U}(f_j)\mathbf{\Sigma}(f_j)[\lambda^{-2}(f_j)+2\lambda^{-1}(f_j)\mathbf{\Sigma}(f_j)+\mathbf{\Sigma}^2(f_j)]^{-1}\mathbf{U}^H(f_j)\bar{\mathbf{a}}(f_j,\theta)}.$$

Review of Wideband Beamspace Capon

- The beamspace method is a preprocessing method that performs spatial filtering by focusing on a region of interest[6].
- Initially was implemented to counteract the effects of low SNR sources and wind noise.
- The $L \times M$ beamspace matrix $\mathbf{B}_{bs}$ is a matrix in $\mathbb{C}^L$ which projects the input from the element space to the beamspace, in $\mathbb{C}^M$, where $L \geq M$.
- A general form of a non-orthogonalized beamspace matrix is

$$\mathbf{B}_{no}(f_j, \theta) = \left[\mathbf{b}(f_j, \phi_{-P} + \theta) \cdots \mathbf{b}(f_j, \phi_0 + \theta) \cdots \mathbf{b}(f_j, \phi_P + \theta)\right], \quad (16)$$

where for an arbitrary array geometry and c the speed of sound

$$\mathbf{b}(f_j, \phi_p) = \begin{bmatrix} e^{j2\pi f_j/c(\alpha_0 \cos(\phi_p) + \beta_0 \sin(\phi_p))} \\ e^{j2\pi f_j/c(\alpha_1 \cos(\phi_p) + \beta_1 \sin(\phi_p))} \\ \vdots \\ e^{j2\pi f_j/c(\alpha_{L-1} cos(\phi_p) + \beta_{L-1} sin(\phi_p))} \end{bmatrix}. \quad (17)$$

Review of Wideband Beamspace Capon

- To ensure orthogonality of the beamspace matrix, we perform

$$\mathbf{B}_{bs} = \mathbf{B}_{no}[\mathbf{B}_{no}^H \mathbf{B}_{no}]^{-\frac{1}{2}} \tag{18}$$

  Clearly, this whitening yields orthogonality in $\mathbf{B}_{bs}^H \mathbf{B}_{bs} = \mathbf{I}_M$.

- The beamspace Capon method results in the weight vector

$$\mathbf{w}_{bs}(f_j, \theta) = \frac{\mathbf{R}_{\mathbf{vv}}^{-1}(f_j, \theta)\mathbf{a}_{bs}(f_j, \theta)}{\mathbf{a}_{bs}^H(f_j, \theta)\mathbf{R}_{\mathbf{vv}}^{-1}(f_j, \theta)\mathbf{a}_{bs}(f_j, \theta)}, \tag{19}$$

  where $\mathbf{R}_{\mathbf{vv}}(f_j, \theta) = \mathbf{B}_{bs}^H(f_j, \theta)\mathbf{R}_{\mathbf{xx}}(f_j)\mathbf{B}_{bs}(f_j, \theta)$ and $\mathbf{a}_{bs}(f_j, \theta) = \mathbf{B}_{bs}^H(f_j, \theta)\mathbf{a}(f_j, \theta)$ are the transformed sample covariance and steering vector, respectively.

- The wideband geometric mean beamspace Capon power spectrum output then becomes

$$P_{G_{bs}}(\theta) = \prod_{j=1}^{J} \frac{1}{\mathbf{a}_{bs}^H(f_j, \theta)\mathbf{R}_{\mathbf{vv}}^{-1}(f_j, \theta)\mathbf{a}_{bs}(f_j, \theta)}.$$

DOA Estimation Results - Baseline Run 1

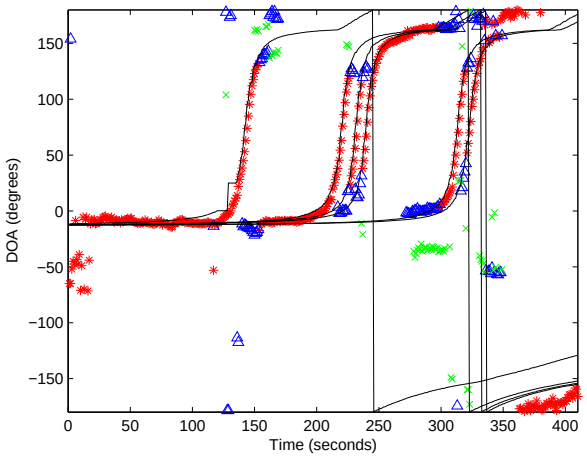

Beamspace Geometric Capon

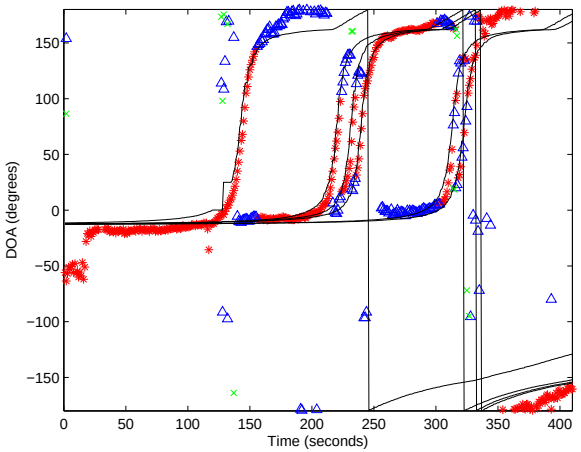

Standard Geometric Capon

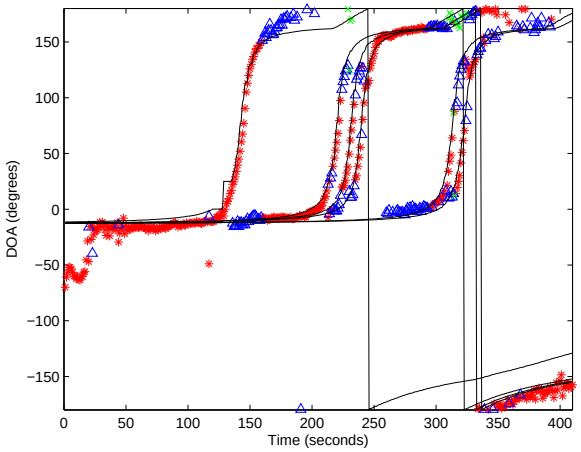

Geometric MUSIC

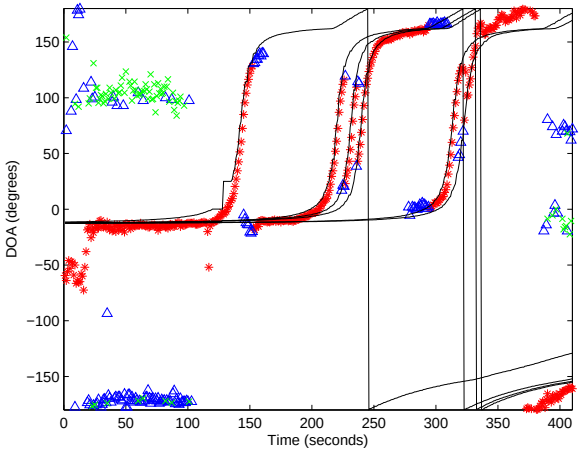

WSF

DOA Estimation Results - Baseline Run 1

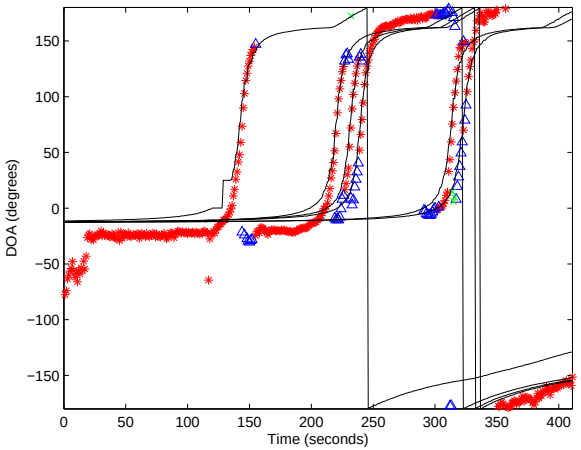

Robust Geometric Capon

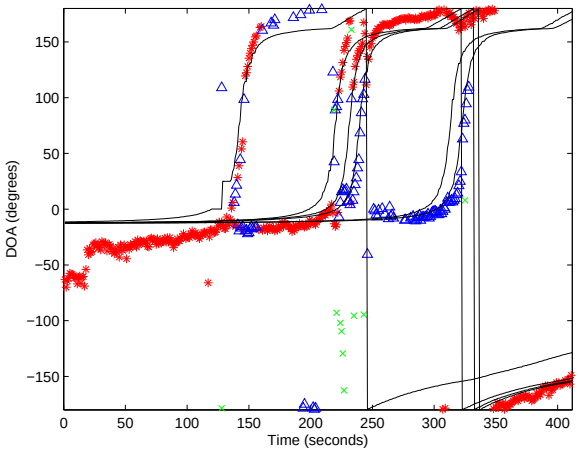

Standard Geometric Capon

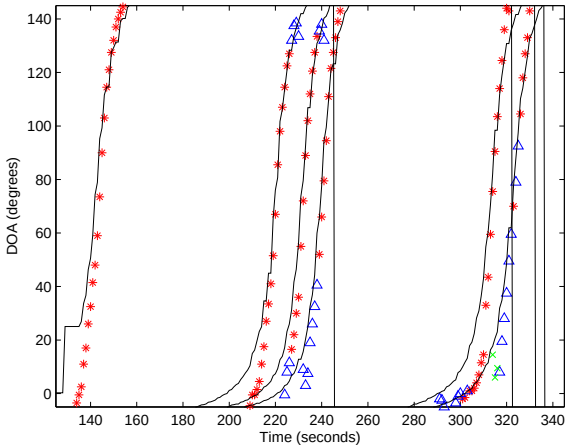

Robust Geometric Capon detail

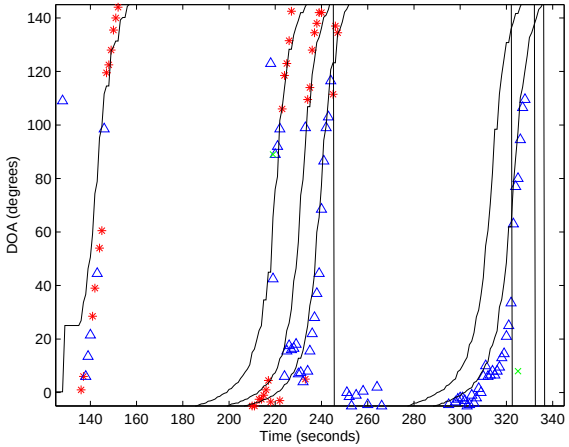

Standard Geometric Capon detail

DOA Estimation Results - Baseline Run 4

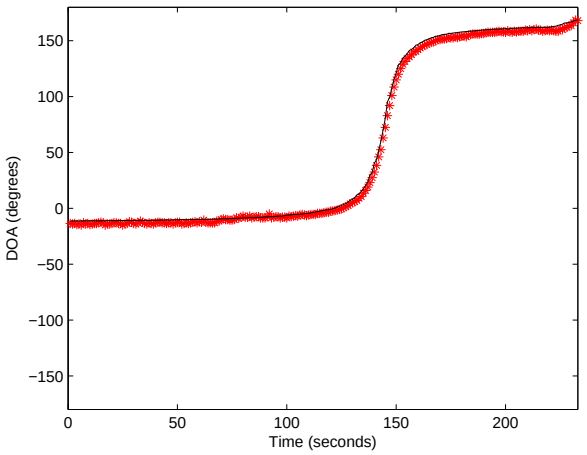

Beamspace Geometric Capon

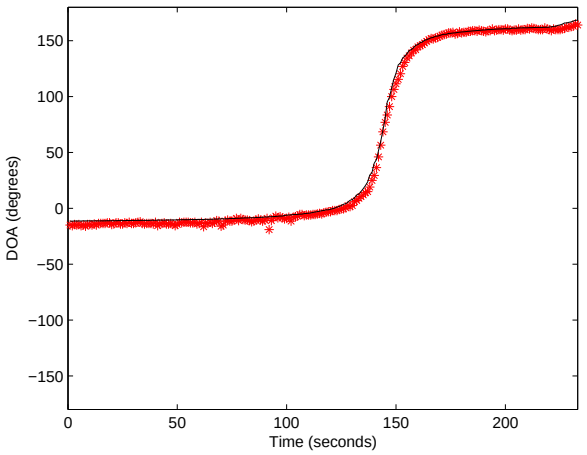

Standard Geometric Capon

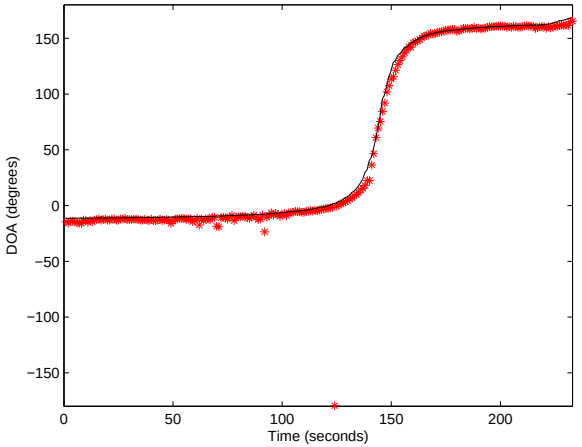

Geometric MUSIC

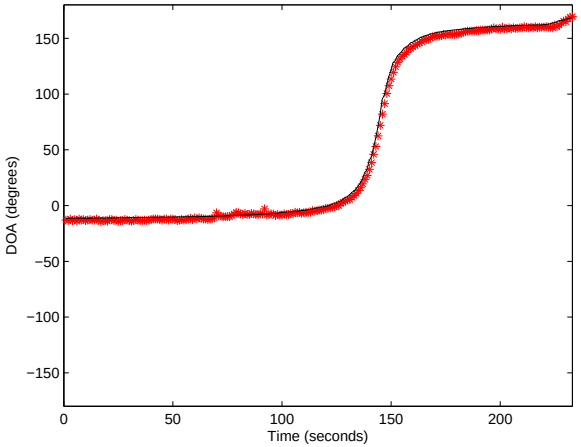

WSF

Error Statistics for Run 4

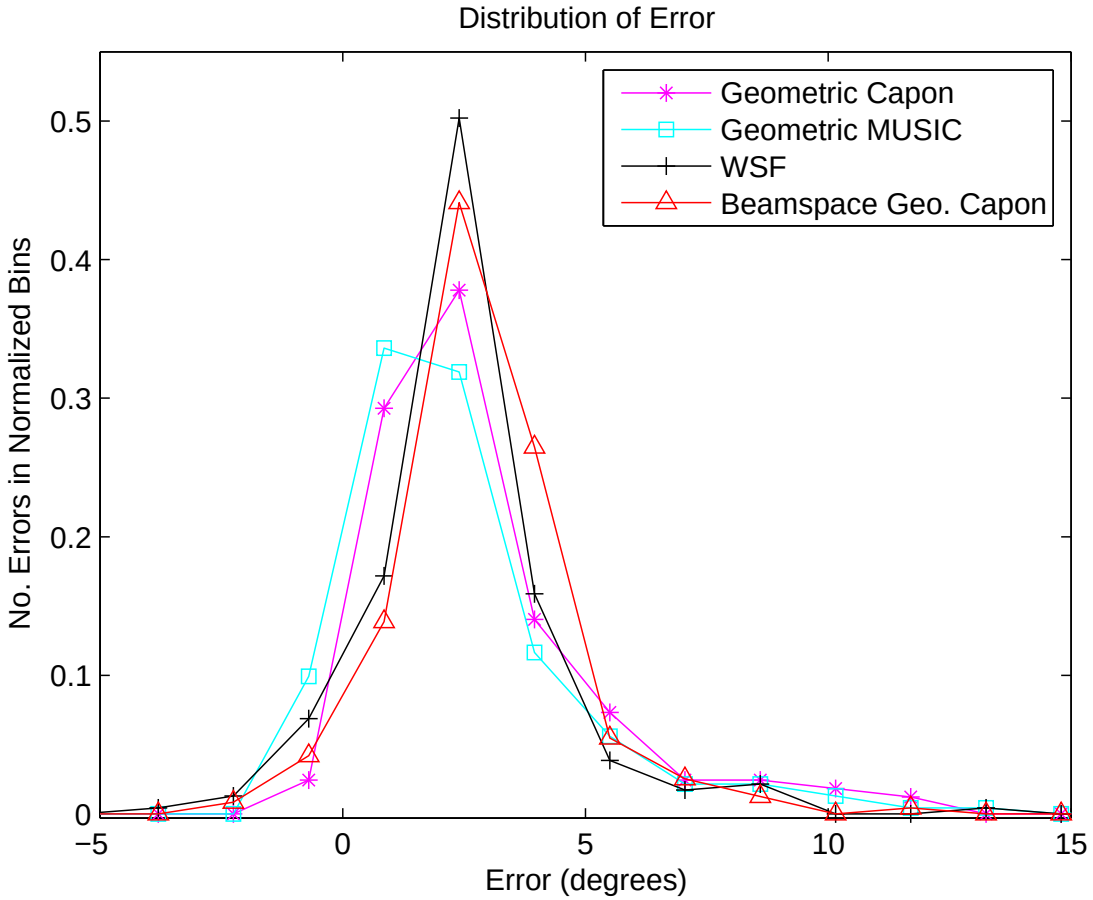

	Geo. Capon	Bmspc Capon	Geo. MUSIC	WSF
μ_e	2.8619°	2.8426°	* 2.5633°	2.6842°
σ_e^2	5.0469	3.3621	6.8435	* 3.0665

DOA Estimation Results - Baseline Run 4

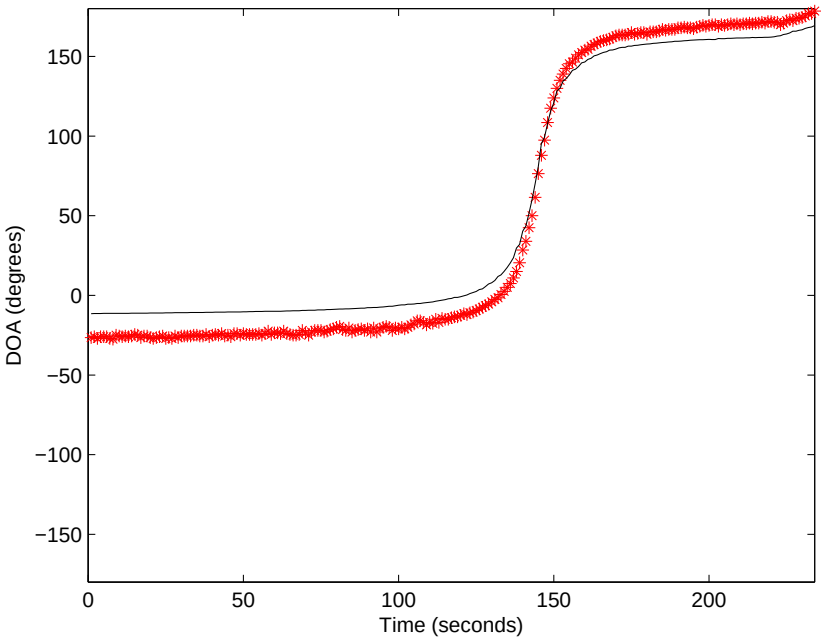

Robust Geometric Capon

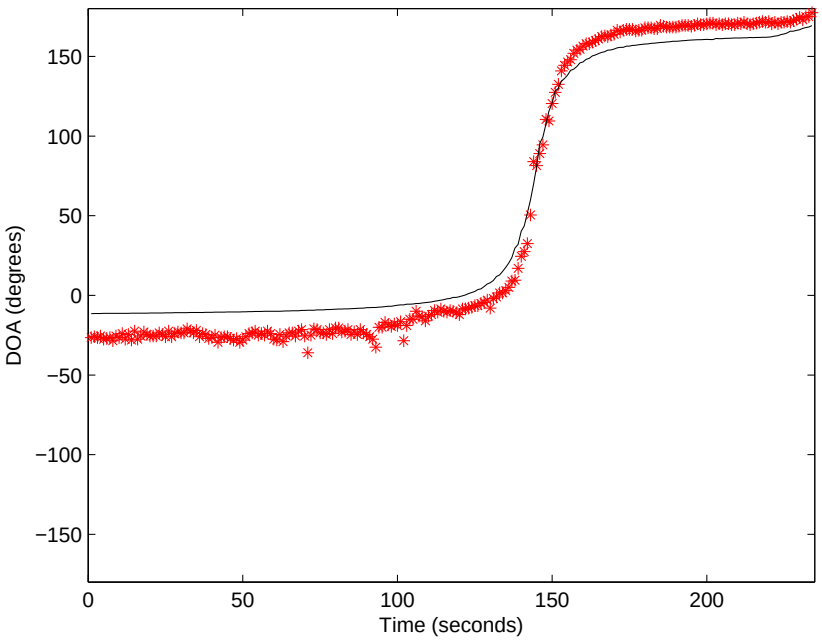

Standard Geometric Capon

Error Statistics for Run 4

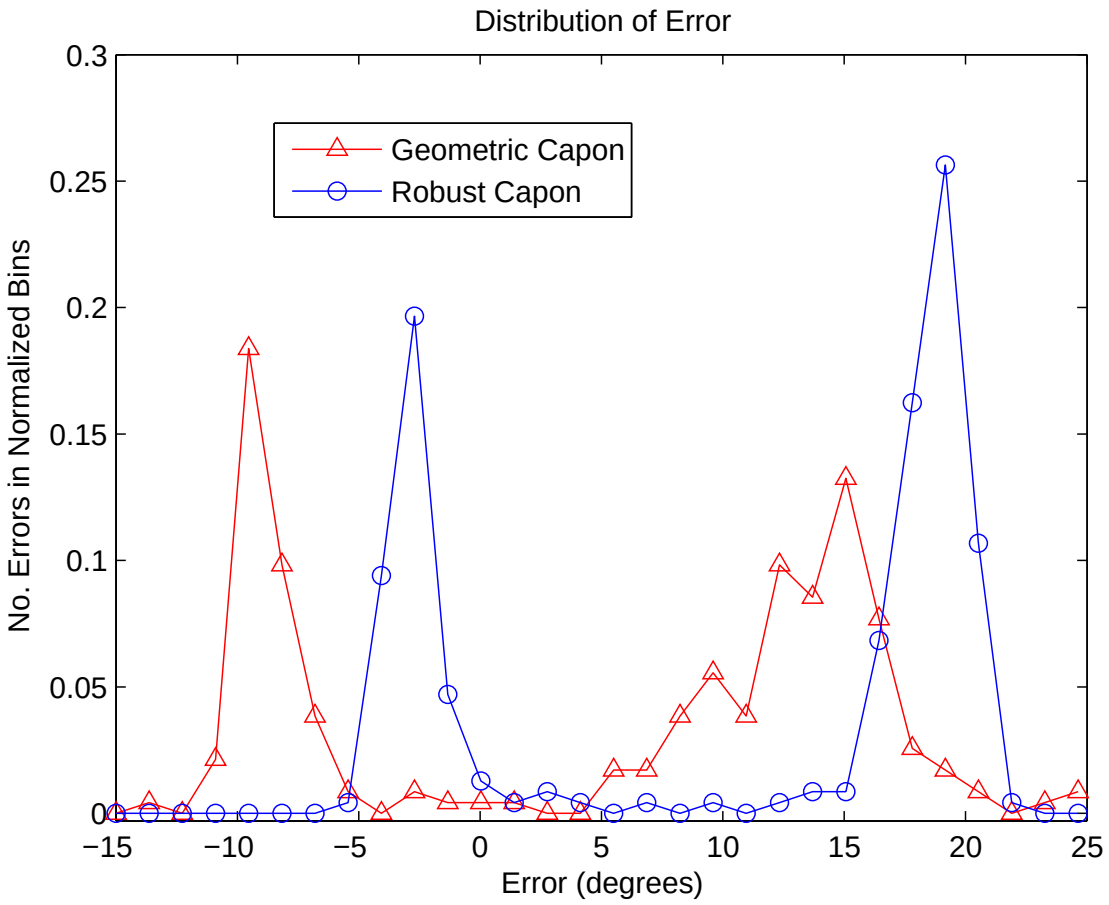

	Geo. Capon	Robust Capon
μ_e	* 5.22°	5.64°
σ_e^2	122.93	* 106.17

DOA Estimation Results - Distributed Run 2

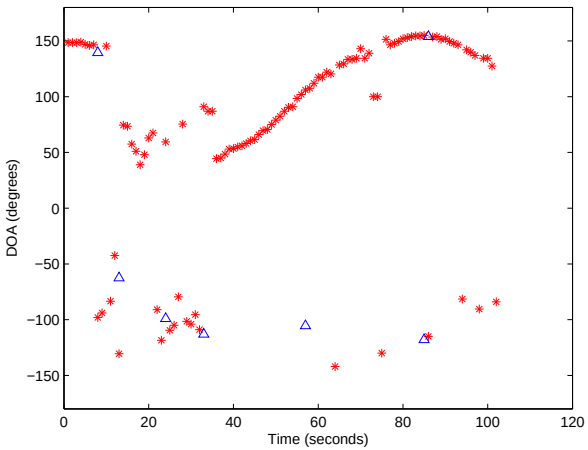

Beamspace Geometric Capon

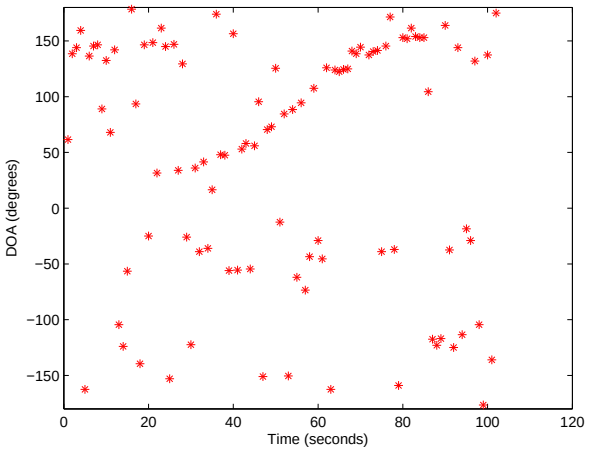

Standard Geometric Capon

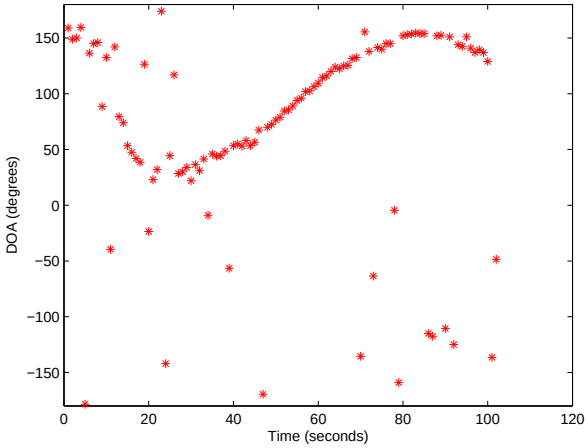

Robust Geometric Capon

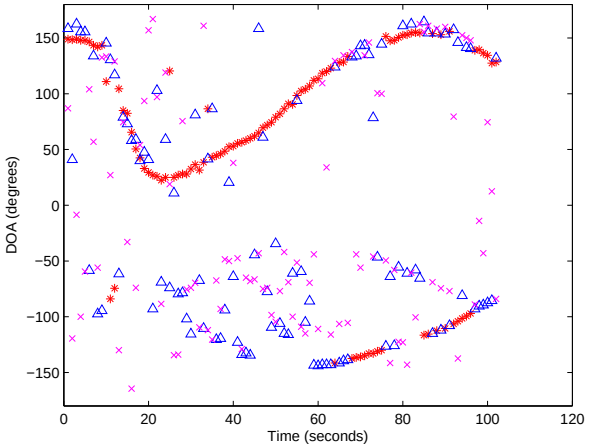

WSF

Outline

Conclusions and Summary

- The tested benchmark algorithms provided good results however, with some drawbacks and deficiencies.
- The error coherence source model enabled the appropriate choice of rank-one robust DOA estimation algorithms.
- The wideband robust Capon provided robust DOA estimates in the presence of sensor location uncertainties and near-field effects.
- Both the wideband beamspace Capon and the robust Capon provided good DOA estimation performance even when there was data loss or corruption.
- Additionally, the beamspace Capon method provided better performance in wind noise and in locating far range sources.

Suggestions for Future Work

- Algorithm for detecting level of coherence and performing DOA estimation with the appropriate matching to whichever error coherence is present.
- Expand the application of these algorithms in this research to other wideband data.
- Explore better ways of finding algorithm parameters, namely, the number of beams and estimated error in the beamspace and robust Capon methods, respectively.
- Using DOA estimation algorithms for providing input to data fusion and tracking methods.

Questions and Thanks

Questions?

- My most sincere an deep thanks to Dr. Azimi for his ideas, editing my writing, and encouragement through this long process.
- Gratitude is also due Dr.'s Scharf and Breidt for their willingness to be members in my committee.
- Also to the members of the signal and image processing laboratory: Bryan, Gordon, Jered, Amanda, Jaime, Makoto, Neil, Derek, Mike and Tim; you have made grad school an interesting and great learning experience.

References I

- T. Pham and B. M. Sadler, “Wideband array processing algorithms for acoustic tracking of ground vehicles,” tech. rep., Army Research Laboratories, Adelphi, MD, 1997.
- M. R. Azimi-Sadjadi, A. Pezeshki, L. Scharf, and M. Hohil, “Wideband DOA estimation algorithms for multiple target detection and tracking using unattended acoustic sensors,” in *Proc. of SPIE’04 Defense and Security Symposium - Unattended Ground Sensors VI*, vol. 5417, pp. 1–11, Apr. 2004.
- M. R. Azimi-Sadjadi, Y. Jiang, and G. Wichern, “Properties of randomly distributed sparse acoustic sensors for ground vehicle tracking and localization,” in *Proc. of SPIE’06 Defense and Security Symposium*, vol. 6201, Apr. 2006.

References II

- T. R. Damarla, J. Chang, and A. Rotolo, “Tracking a convoy of multiple targets using acoustic sensor data,” in *Proc. of SPIE’03 Defense and Security Symposium - Acquisition, Tracking, and Pointing XVII*, vol. 5082, pp. 37–42, Aug. 2003.
- M. E. Hohil, J. R. Heberley, J. Chang, and A. Rotolo, “Vehicle counting and classification algorithms for unattended ground sensors,” in *Proc. of SPIE’03 Defense and Security Symposium - Unattended Ground Sensor Technologies and Applications V*, pp. 99–110, Sept. 2003.
- H. L. V. Trees, *Optimum Array Processing*. Wiley Interscience, 2002.

References III

- R. O. Schmidt, “Multiple emitter location and signal parameter estimation,” *IEEE Trans. on Antennas and Propagation*, vol. 34, pp. 276 – 280, Mar. 1986.
- M. Viberg and B. Ottersten, “Sensor array processing based on subspace fitting,” *IEEE Trans. on Signal Processing*, vol. 39, pp. 1110–1121, May 1991.
- J. Krolik and D. Swingler, “Multiple broad-band source location using steered covariance matrices,” *IEEE Trans. on Aoustics, Speech, and Signal Processing*, vol. 37, pp. 1481–1494, Oct. 1989.

References IV

- J. Krolik, *Focused wideband Array Processing for Spatial Spectral Estimation*, ch. 6.
  in “Advances in Spectrum Analysis and Array Processing, Vol. II”, Prentice-Hall, 1991.
- T. Pham and M. Fong, “Real-time implementation of MUSIC for wideband acoustic detection and tracking,” in *Proc. of SPIE AeroSense’97 - Automatic Target Recognition VII*, vol. 3069, pp. 250–256, Apr. 1997.
- H. Wang and M. Kaveh, “Coherent signal-subspace processing for the detection and estimation of angles of arrival of multiple wide-band sources,” *IEEE Trans. on Acoustics, Speech, and Signal Processing*, vol. 33, pp. 823 – 831, Aug. 1985.

References V

- E. D. D. Claudio and R. Parisi, “WAVES: Weighted average of signal subspaces for robust wideband direction finding,” *IEEE Trans. on Signal Processing*, vol. 49, pp. 2179–2191, Oct. 2001.
- A. L. Swindlehurst and M. Viberg, “Bayesian approaches for robust array signal processing.” research supported by NSF grant MIP-9408154, 1991.
- D. Asztély, “Spatial models for narrowband signal estimation with antenna arrays,” tech. lic. thesis, Royal Institute of Technology, Stockholm, Sweden, Nov. 1997.
- D. Asztély, B. Ottersten, and A. L. Swindlehurst, “Generalised array manifold model for wireless communication channels with local scattering,” *IEE Proc.-Radar, Sonar Navig.*, vol. 145, pp. 51–57, Feb. 1998.

References VI

- S. Valaee, B. Champagne, and P. Kabal, “Parametric localization of distributed sources,” *IEEE Trans. on Signal Processing*, vol. 43, pp. 2144 – 2153, Sept. 1995.
- A. Pezeshki, B. D. V. Veen, L. L. Scharf, H. Cox, and M. Lundberg, “Eigenvalue beamforming using a multi-rank MVDR beamformer and subspace selection,” *to appear in IEEE Trans. on Signal Processing*, submitted Sept. 2006.
- L. L. Scharf, A. Pezeshki, and M. Lundberg, “Multi-rank adaptive beamforming,” in *Proc. IEEE 13th Workshop Statistical Signal Processing*, (Bordeaux, France), July 2005.

References VII

- Y. Meng, P. Stoica, and K. M. Wong, "Estimation of the directions of arrival of spatially dispersed signals in array processing," in *Proceedings of IEE Conf. on Radar, Sonar, and Navig.*, vol. 143, Feb. 1996.
- J. Li, P. Stoica, and Z. Wang, "On robust capon beamforming and diagonal loading," *IEEE Trans. on Signal Processing*, vol. 51, pp. 1702–1715, July 2003.

Other Wideband Algorithm Power Spectrums

The wideband arithmetic mean Capon power spectrum is

$$P_A(\theta) = \sum_{j=1}^{J} p(f_j, \theta) = \sum_{j=1}^{J} \frac{1}{\mathbf{a}^H(f_j, \theta)\mathbf{R}_{\mathbf{xx}}^{-1}(f_j)\mathbf{a}(f_j, \theta)} \tag{20}$$

The wideband harmonic mean Capon power spectrum is

$$P_H(\theta) = \frac{1}{\sum_{j=1}^{J} \mathbf{w}^H(f_j, \theta)\mathbf{R}_{\mathbf{xx}}(f_j)\mathbf{w}(f_j, \theta)} \tag{21}$$

The WSF power spectrum is

$$P_{WSF}(\theta) = \frac{1}{tr\{\sum_{j=1}^{J} \mathbf{P}_{\mathbf{A}_1}^{\perp}(f_j, \theta)\mathbf{U}_s(f_j)\mathbf{W}(f_j)\mathbf{W}^H(f_j)\mathbf{U}_s^H(f_j)\mathbf{P}_{\mathbf{A}_1}^{\perp}(f_j, \theta)\}}, \tag{22}$$

where $\mathbf{P}_{\mathbf{A}_1}(f_j, \theta) = \mathbf{a}(f_j, \theta)\mathbf{a}^{\dagger}(f_j, \theta)$ is the rank-one projection matrix.

Derivation of Arithmetic Mean Wideband Capon I

The wideband arithmetic Capon problem can be cast as

$$\begin{aligned} \min_{w(f_j,\theta)} \quad P_A(\theta) &= \sum_{j=1}^{J} \sum_{k=1}^{K} \mathbf{w}^H(f_j,\theta)\mathbf{x}(f_j,k)\mathbf{x}^H(f_j,k)\mathbf{w}(f_j,\theta) \\ &= \sum_{j=1}^{J} \mathbf{w}^H(f_j,\theta)\mathbf{R}_{\mathbf{xx}}(f_j)\mathbf{w}(f_j,\theta) \end{aligned} \tag{23}$$

under the constraints

$$\mathbf{w}^H(f_j,\theta)\mathbf{a}(f_j,\theta) = 1, \quad \forall j \in [1,J] \tag{24}$$

It is assumed that $\mathbf{w}(f_j,\theta)$ is independent of k within the observation period T_0. This leads to a constrained minimization problem

$$\min_{w(f_j,\theta)} \left(\sum_{j=1}^{J} \mathbf{w}^H(f_j,\theta)\mathbf{R}_{\mathbf{xx}}(f_j)\mathbf{w}(f_j,\theta) + \sum_{j=1}^{J} \lambda(f_j)(\mathbf{w}^H(f_j,\theta)\mathbf{a}(f_j,\theta) - 1) \right) \tag{25}$$

Derivation of Arithmetic Mean Wideband Capon II

where $\lambda(f_j)$'s are frequency dependent Lagrange multipliers. This minimization problem leads the optimal beamformer, but here this optimization produces J narrowband rank-one Capon beamformers for $\mathbf{w}(f_j, \theta)$'s,

$$\mathbf{w}(f_j, \theta) = \frac{\mathbf{R}_{\mathbf{xx}}^{-1}(f_j)\mathbf{a}(f_j, \theta)}{\mathbf{a}^H(f_j, \theta)\mathbf{R}_{\mathbf{xx}}^{-1}(f_j)\mathbf{a}(f_j, \theta)}, \quad \forall j \in [1, J] \tag{26}$$

and the wideband Capon spectrum,

$$P_A(\theta) = \sum_{j=1}^{J} p(f_j, \theta) = \sum_{j=1}^{J} \frac{1}{\mathbf{a}^H(f_j, \theta)\mathbf{R}_{\mathbf{xx}}^{-1}(f_j)\mathbf{a}(f_j, \theta)} \tag{27}$$

MUltiple SIgnal Classification (MUSIC)

The MUSIC algorithm is a type of subspace-based algorithm which uses the decomposition of the orthogonal (or unitary for this complex case) signal and noise subspaces some eigendecomposition

$$\mathbf{R_{xx}}(f_j) = \mathbf{U_s}(f_j)\mathbf{\Sigma_s}(f_j)\mathbf{U_s^H}(f_j) + \mathbf{U_n}(f_j)\mathbf{\Sigma_n}(f_j)\mathbf{U_n^H}(f_j). \tag{28}$$

Thus, the squared Euclidean distance between the steering vector $\mathbf{a}(f_j, \theta)$ and the noise subspace,

$$\partial^2 = \mathbf{a}^H(f_j, \theta)\mathbf{U_n}(f_j)\mathbf{U_n^H}(f_j)\mathbf{a}(f_j, \theta), \tag{29}$$

will be minimum in the direction of a source. The incoherent wideband geometric mean MUSIC algorithm is formulated by the inverse of this distance as

$$P_{MUSIC_G}(\theta) = \prod_{j=1}^{J} p_{MUSIC}(f_j, \theta) = \prod_{j=1}^{J} \frac{1}{\mathbf{a}^H(f_j, \theta)\mathbf{U}_n(f_j)\mathbf{U}_n^H(f_j)\mathbf{a}(f_j, \theta)}.$$

Weighted Subspace Fitting (WSF)

Narrowband subspace fitting attempts to fit the data to a search array manifold as the minimization problem

$$\min_{\boldsymbol{\theta}} ||\mathbf{x}(f_j,k) - \mathbf{A}(f_j,\boldsymbol{\theta})\mathbf{s}(f_j,k)||_F^2. \tag{30}$$

the signal estimate is

$$\hat{\mathbf{s}}(f_j,k) = \mathbf{A}^{\dagger}(f_j,\boldsymbol{\theta})\mathbf{x}(f_j,k), \tag{31}$$

The error in this LS estimation of the signal estimate is given by

$$\mathbf{e}(f_j,k) = \mathbf{x}(f_j,k) - \mathbf{A}(f_j,\boldsymbol{\theta})\hat{\mathbf{s}}(f_j,k) = \mathbf{P}_{\mathbf{A}}^{\perp}(f_j,\boldsymbol{\theta})\mathbf{x}(f_j,k) \tag{32}$$

where

$$\mathbf{P}_{A}^{\perp}(f_j,\boldsymbol{\theta}) = \mathbf{I} - \mathbf{P}_{\mathbf{A}}(f_j,\boldsymbol{\theta}) = \mathbf{I} - \mathbf{A}(f_j,\boldsymbol{\theta})[\mathbf{A}^H(f_j,\boldsymbol{\theta})\mathbf{A}(f_j,\boldsymbol{\theta})]^{-1}\mathbf{A}^H(f_j,\boldsymbol{\theta}) \tag{33}$$

is the orthogonal projection complement operator onto the subspace spanned by the columns of the array response matrix $\mathbf{A}(f_j,\boldsymbol{\theta})$.

Weighted Subspace Fitting (WSF)

The algorithm is a multi-dimensional search through $\boldsymbol{\theta}$ for the minimum of the squared error between this estimate and the actual signal,

$$\boldsymbol{\theta} = \arg\min_{\boldsymbol{\theta}} tr\{\sum_{j=1}^{J} \mathbf{P}_{\mathbf{A}}^{\perp}(f_j,\theta)\mathbf{R}_{\mathbf{xx}}(f_j)\mathbf{P}_{\mathbf{A}}^{\perp}(f_j,\theta)\}. \tag{34}$$

The decomposition of $\mathbf{R}_{\mathbf{xx}}(f_j)$ allows it to be written approx. as

$$\mathbf{R}_{\mathbf{xx}}(f_j) \approx \mathbf{U}_{\mathbf{s}}(f_j)\boldsymbol{\Sigma}_s(f_j)\mathbf{U}_{\mathbf{s}}^H(f_j). \tag{35}$$

The algorithm generalizes this decomposition as

$$\mathbf{R}_{\mathbf{xx}}(f_j) \approx \mathbf{U}_{\mathbf{s}}(f_j)\mathbf{W}(f_j)\mathbf{W}^H(f_j)\mathbf{U}_{\mathbf{s}}^H(f_j), \tag{36}$$

where the weighting matrix, $\mathbf{W}(f_j) = (\boldsymbol{\Sigma}_{\mathbf{s}}(f_j) - \sigma_{\mathbf{n}}^2\mathbf{I})\boldsymbol{\Sigma}\_s^{-1/2}(f_j)$, is commonly used. The weighted subspace replaces $\mathbf{R}_{\mathbf{xx}}(f_j)$ and the multi-dimensional search becomes

$$\boldsymbol{\theta} = \arg\min_{\boldsymbol{\theta}} tr\{\sum_{j=1}^{J} \mathbf{P}_{\mathbf{A}}^{\perp}(f_j,\boldsymbol{\theta})\mathbf{U}_s(f_j)\mathbf{W}(f_j)\mathbf{W}^H(f_j)\mathbf{U}_s^H(f_j)\mathbf{P}_{\mathbf{A}}^{\perp}(f_j,\boldsymbol{\theta})\}.$$

STeered Covariance Matrix (STCM) Method

- The desired effect of the STCM algorithm is to generate a single coherent signal subspace by focusing to a reference frequency those subspaces at other frequencies.
- Focusing matrices $\mathbf{T}(f_j, \theta), j = 1, 2, ..., J$, exist so that

$$\mathbf{T}(f_j, \theta)\mathbf{A}(f_j, \theta) = \mathbf{A}(f_0, \theta), \quad s.t.\ \mathbf{T}(f_j, \theta)\mathbf{T}^H(f_j, \theta) = \mathbf{I}. \tag{37}$$

- The steered or focused spatial covariance matrix may therefore be defined as

$$\mathbf{R}(\theta) = \sum_{j=1}^{J} \mathbf{R}(f_j, \theta) = \sum_{j=1}^{J} \mathbf{T}(f_j, \theta)\mathbf{R}_{\mathbf{xx}}(f_j)\mathbf{T}^H(f_j, \theta) \tag{38}$$

STeered Covariance Matrix (STCM) Method

- Using the array signal model, we can rewrite $\mathbf{R}(\theta)$ as

$$\mathbf{R}(\theta) = \sum_{j=1}^{J} \mathbf{A}(f_0, \theta)\mathbf{R_s}(f_j)\mathbf{A}^H(f_0, \theta) + \mathbf{R_{n_\theta}}. \tag{39}$$

  $\mathbf{R_{n_\theta}}$ is the focused noise covariance.
- The STCM focusing method can be *applied in tandem* with any other narrowband DOA estimation algorithm, as its results in a single covariance matrix.

Array Geometries

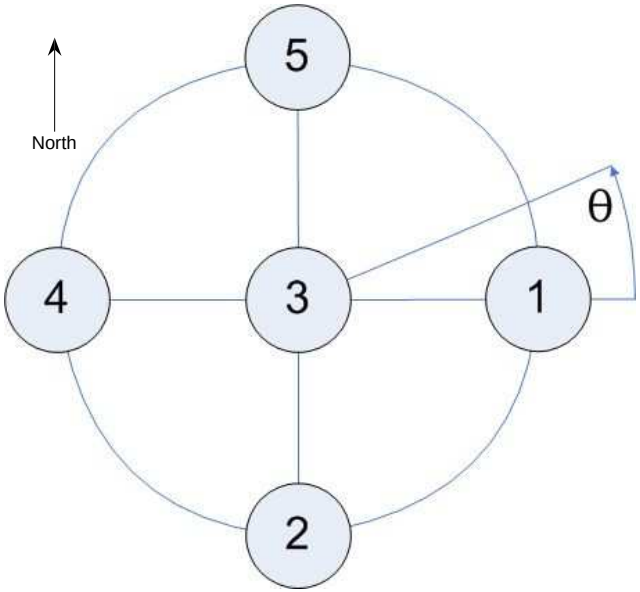

Baseline array

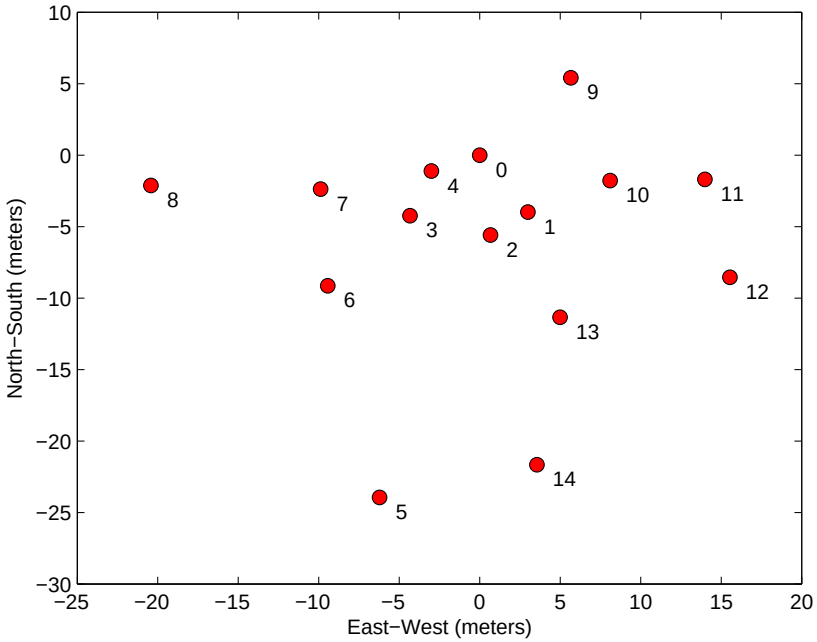

Distributed array

Examples of Vehicle Movement and Acoustic Data: Baseline Array

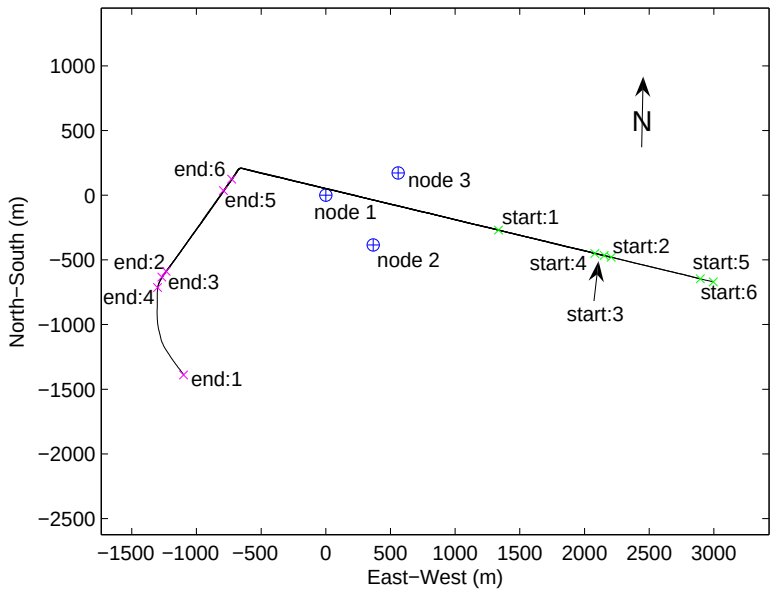

Movement path baseline Run 1

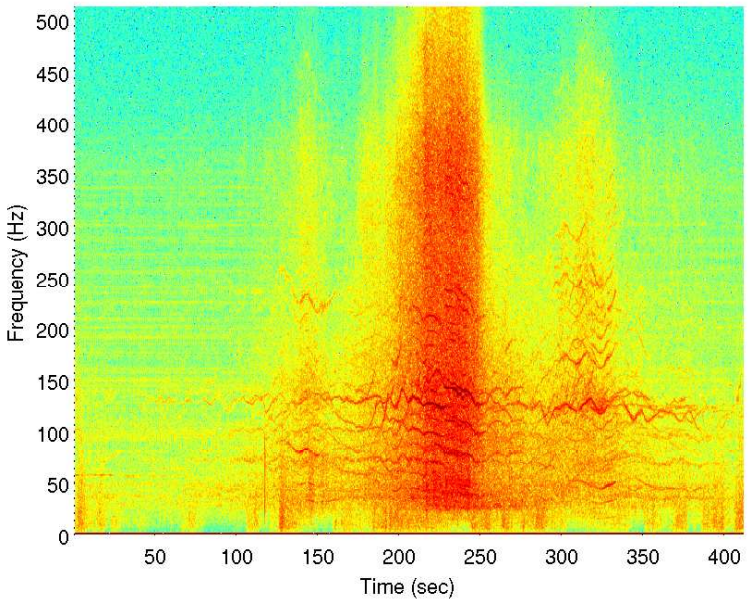

Spectrogram of mic 0, baseline Run 1

Examples of Vehicle Movement and Acoustic Data: Distributed Array

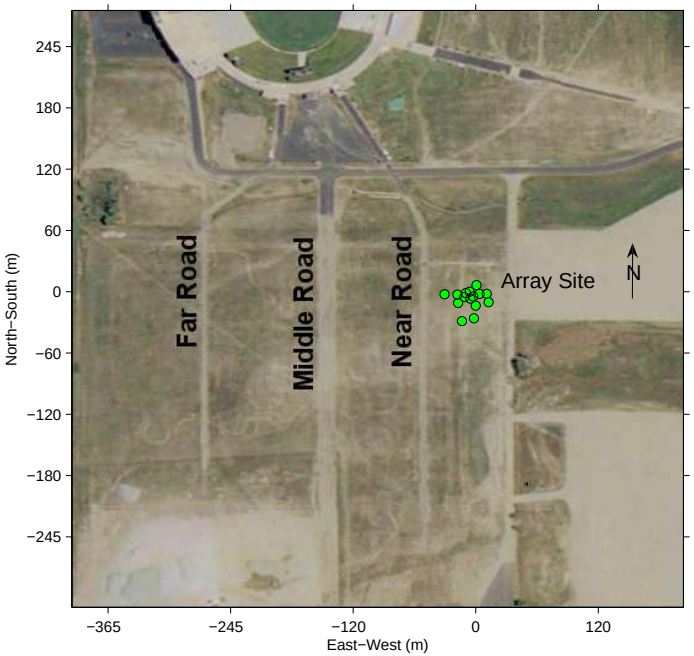

Data collection site

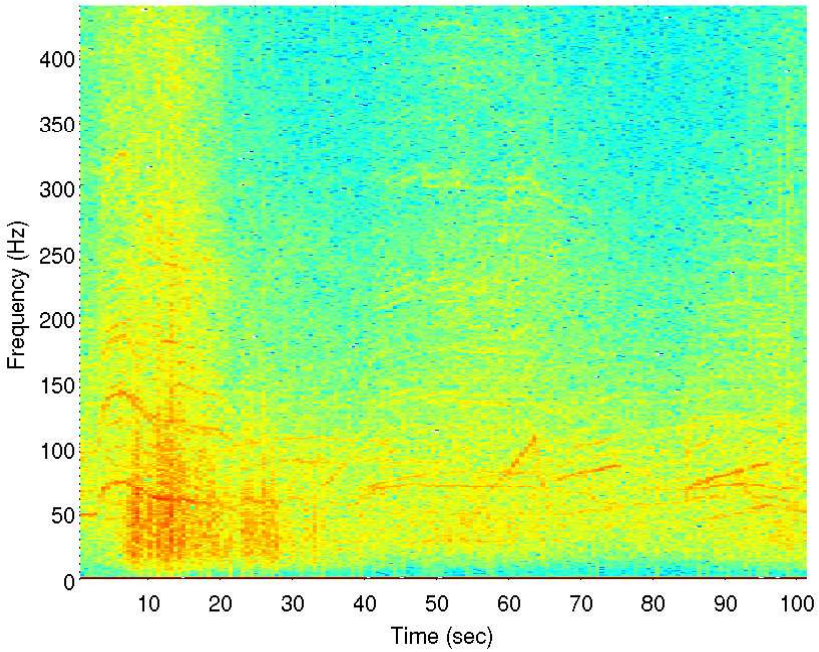

Spectrogram of mic 0, distributed Run 2

Bad Time-series Data

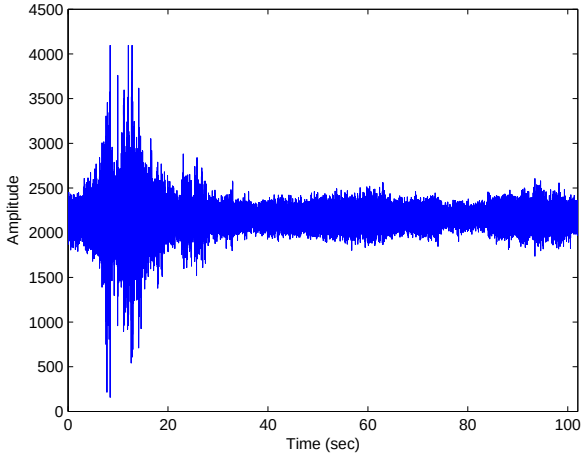

Working node

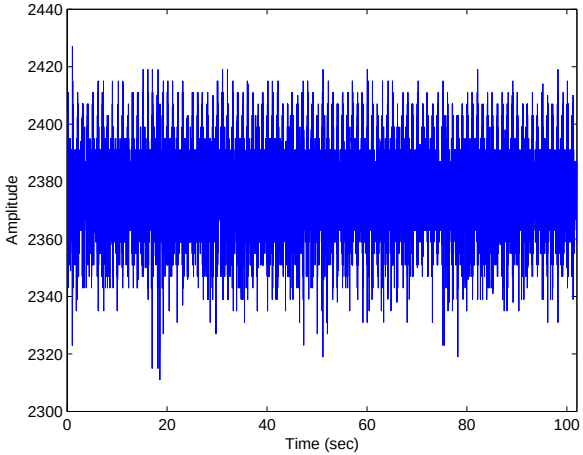

Bad mic amplifier node

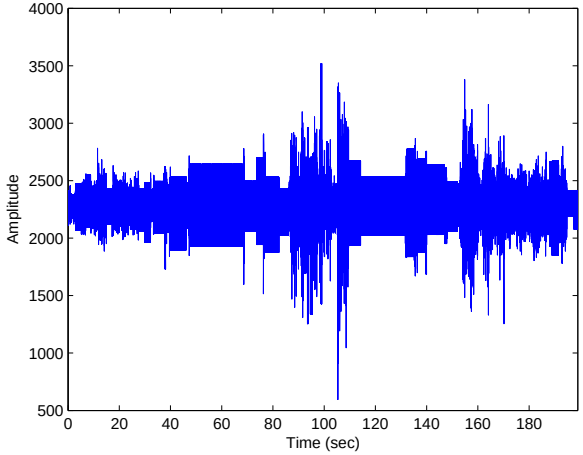

Missing data node

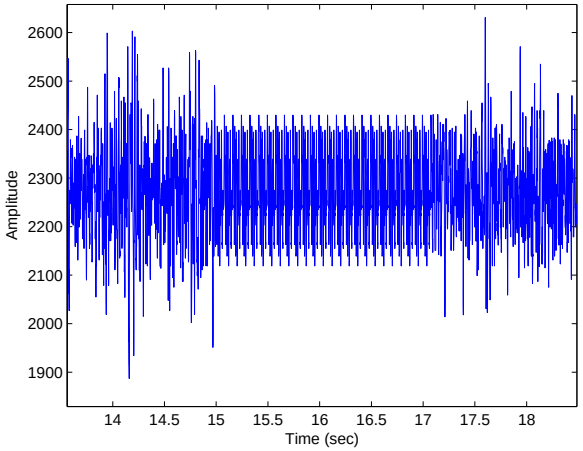

Detail of missing data node

Bearing Response Analysis - Baseline Array

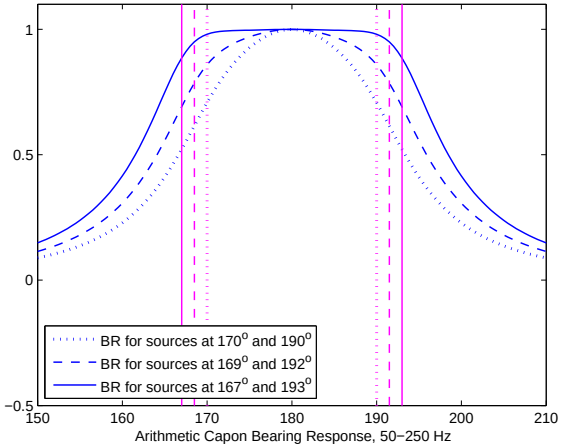

Arithmetic Capon

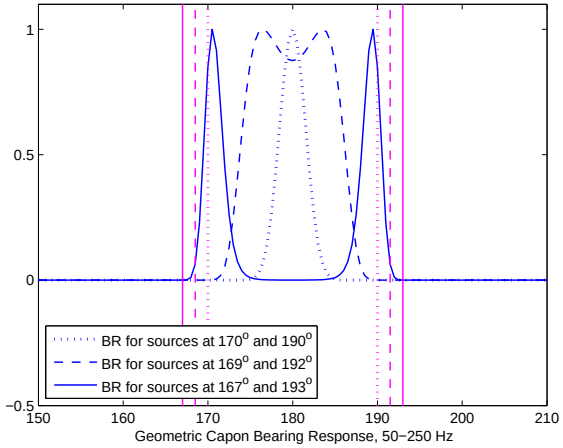

Geometric Capon

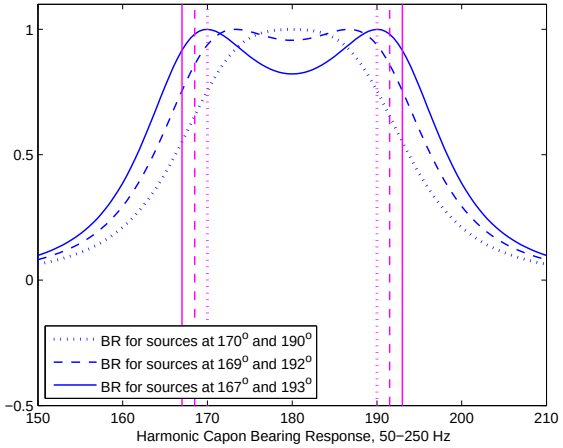

Harmonic Capon

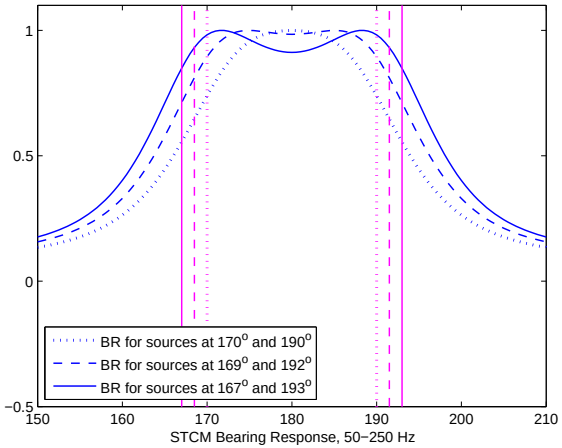

STCM

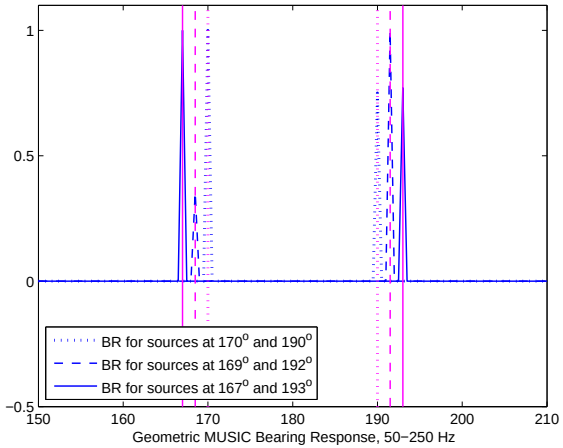

Geometric MUSIC

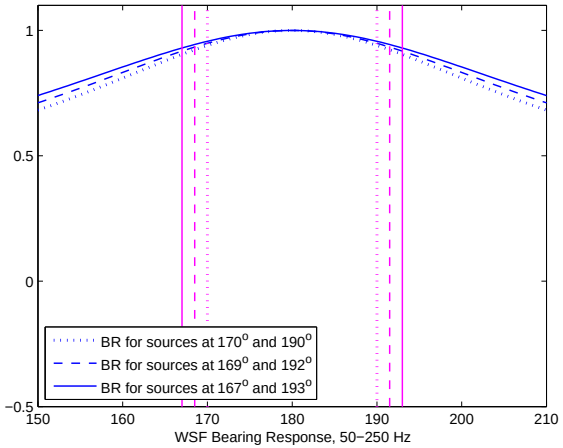

WSF

5-element circular array with two sources at separations of 20°, 23°, and 26°.

New Alg. Bearing Response Analysis - Baseline Array

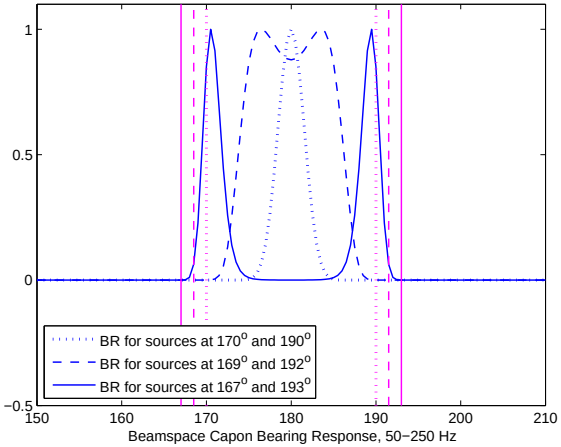

Beamspace Geometric Capon

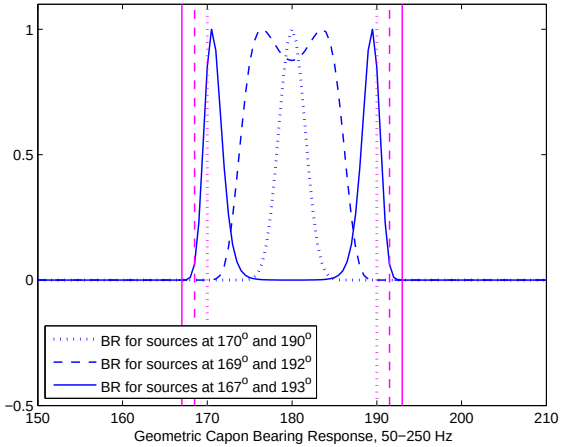

Standard Geometric Capon

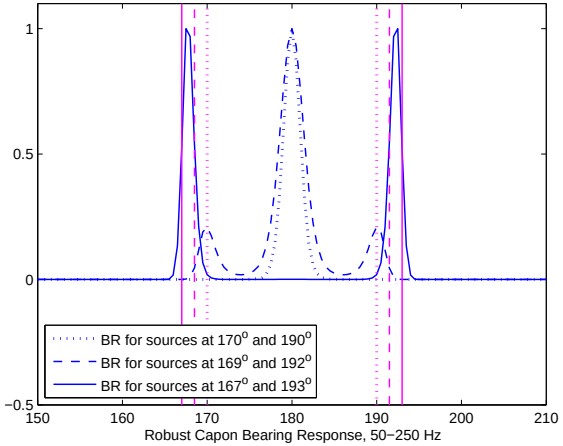

Robust Geometric Capon

5-element circular array with two sources at separations of 20°, 23°, and 26°.

Bearing Response Analysis - Random Array

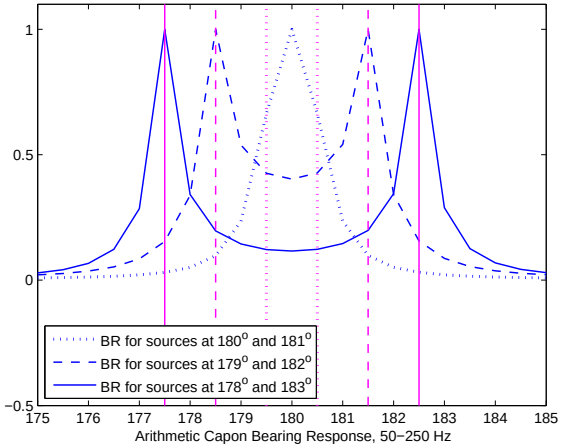

Arithmetic Capon

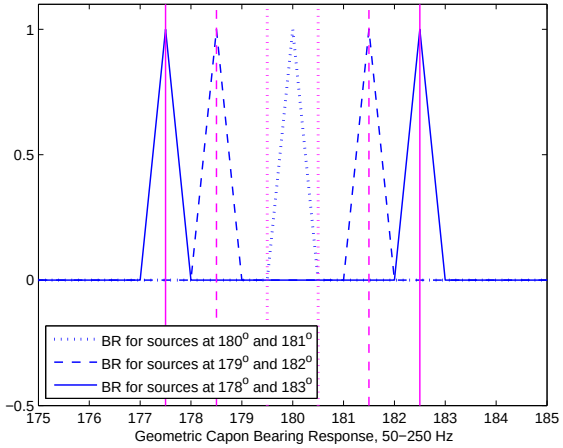

Geometric Capon

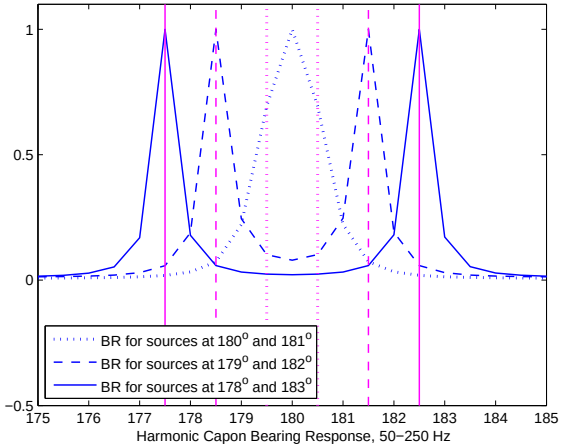

Harmonic Capon

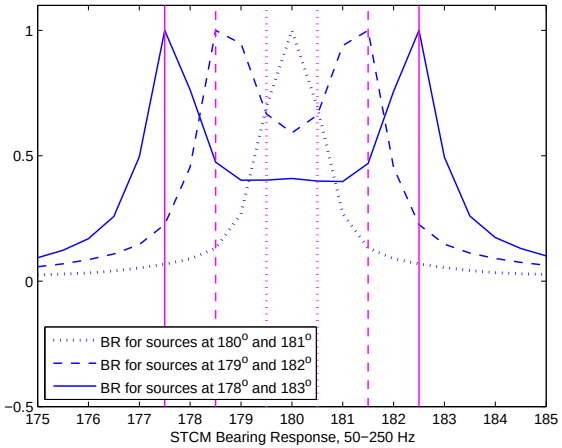

STCM

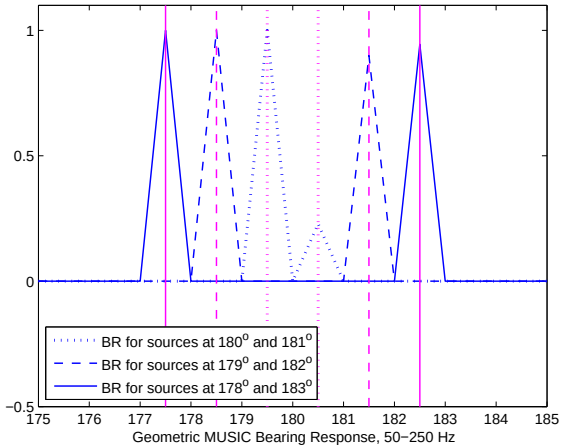

Geometric MUSIC

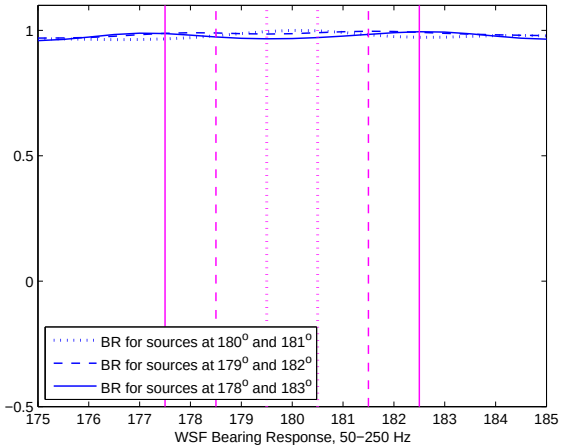

WSF

15-element randomly distributed array with two sources at separations of 1°, 3°, and 4°.

New Alg. Bearing Response Analysis - Random Array

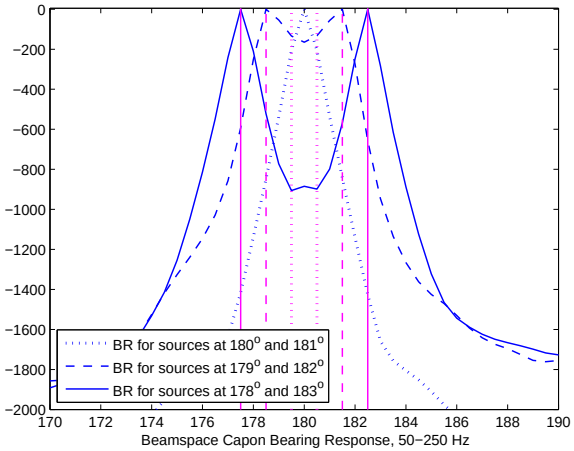

Beamspace Geometric Capon

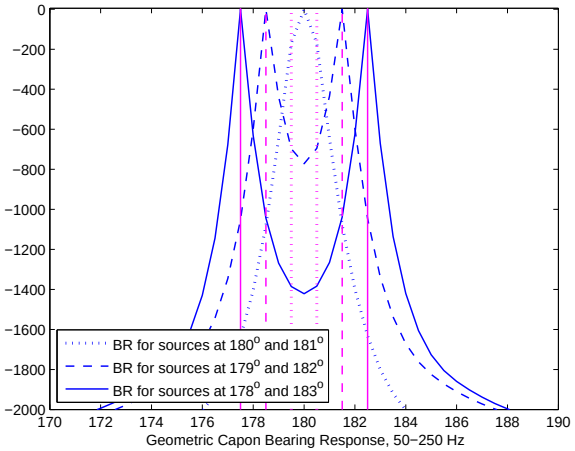

Standard Geometric Capon

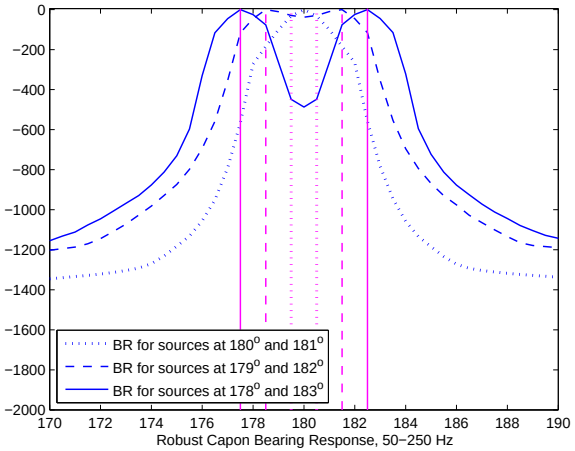

Robust Geometric Capon

15-element randomly distributed array with two sources at separations of 1°, 3°, and 4°.

Spatially Coherent Signals

Coherent sources includes slow fading multipath, near-field effects, and even the arrays errors discussed previously. In this case the spatial dependent signal density is given by

$$s_i(f_j, \phi; \boldsymbol{\psi}_i) = \gamma_i(f_j) g(f_j, \phi; \boldsymbol{\psi}_i) \tag{40}$$

which results in the angular auto correlation

$$p(f_j, \phi, \phi'; \boldsymbol{\psi}) = \eta(f_j,) g(f_j, \phi; \boldsymbol{\psi}) g^*(f_j, \phi'; \boldsymbol{\psi}) \tag{41}$$

with $\eta(f_j) = E\{\gamma(f_j)\gamma^*(f_j)\}$. The integral is separable as

$$\begin{aligned} \mathbf{R}_i(f_j, \boldsymbol{\psi}_i) &= \int_{\phi \in \Phi} \int_{\phi' \in \Phi} \mathbf{a}(f_j, \phi) p_i(f_j, \phi, \phi'; \boldsymbol{\psi}_i) \mathbf{a}^H(f_j, \phi') d\phi d\phi' \\ &= \eta_i \int_{\phi \in \Phi} \mathbf{a}(f_j, \phi) g(f_j, \phi; \boldsymbol{\psi}_i) d\phi \int_{\phi' \in \Phi} g^*(f_j, \phi'; \boldsymbol{\psi}_i) \mathbf{a}^H(f_j, \phi') d\phi'. \end{aligned}$$

and demonstrates that the coherent signal is rank-one.

Illustration of Coherent Signal

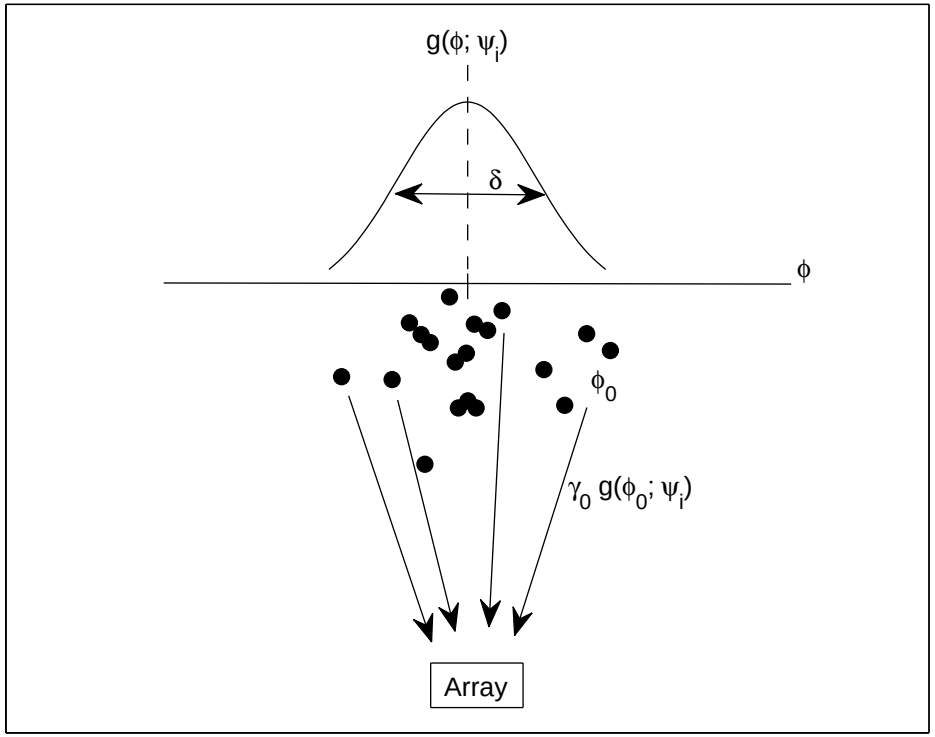

Illustration of distributed source with spatial coherence.

Spatially Incoherent Sources

An incoherent signal exists when the signal rays arriving from different directions can be assumed uncorrelated. The angular auto-correlation is written as

$$p(f_j, \phi, \phi'; \boldsymbol{\psi}) = p(f_j, \phi; \boldsymbol{\psi})\delta(\phi - \phi') \tag{42}$$

The noise-free array correlation matrix for this signal is

$$\mathbf{R}_i(f_j, \boldsymbol{\psi}) = \int_{\phi \in \Phi} \mathbf{a}(f_j, \phi) p_i(f_j, \phi; \boldsymbol{\psi}_i) \mathbf{a}^H(f_j, \phi) d\phi. \tag{43}$$

This incoherent source covariance $\mathbf{R}_i(f_j, \boldsymbol{\psi}_i)$ is always full rank. Using an approximation to the full rank representation is practical for many distributions (and spreading widths).

Partially Incoherent Sources

As a simple example consider the uniform distribution on $[-\frac{\varepsilon}{2}, \frac{\varepsilon}{2}]$ which results in the covariance

$$\begin{aligned} \mathbf{R}_s(\psi_i) &= \int_{\phi\in\Phi} p_i(\phi;\psi_i)\mathbf{a}(\phi)\mathbf{a}^H(\phi)d\phi \\ &= \frac{1}{\varepsilon}\int_{-\varepsilon/2}^{\varepsilon/2} \mathbf{a}(\phi)\mathbf{a}^H(\phi)d\phi \\ &\approx \sigma_{\mathbf{s}}^2\mathbf{U}_{\mathbf{s}}\mathbf{\Lambda}\mathbf{U}_{\mathbf{s}}^H, \end{aligned} \tag{44}$$

where $\mathbf{rank}(\mathbf{R_s}) \approx \frac{\varepsilon}{2\pi}L = p$. The matrix $\mathbf{U}_s$ is the $L \times p$ basis for the p dimensional subspace $\langle \mathbf{U}_s \rangle$ and $\mathbf{\Lambda} \approx \mathbf{I}$, i.e. signal power is even across all distributed components.

Partially Incoherent Sources

So the generation of a input sample, **x**, for an partially incoherent noise-free source looks like

$$\begin{aligned} \mathbf{x} &= \mathbf{U_s b} s \\ E[\mathbf{b}\mathbf{b}^H] &= \mathbf{\Lambda}_s \\ E[ss^*] &= \sigma_{\mathbf{s}}^2 \\ \mathbf{R}_s &= E[\mathbf{x}\mathbf{x}^H] = \sigma_s^2 \mathbf{U}_s \mathbf{\Lambda}_s \mathbf{U}_s^H, \end{aligned} \tag{45}$$

where every sample within the observation period is formed from a random linear combination of the p signal subspace basis vectors. The coherent source is a similar formulation, except that the random combining vector **b** is fixed for the observation period.

DOA Estimation Results - Baseline Run 3

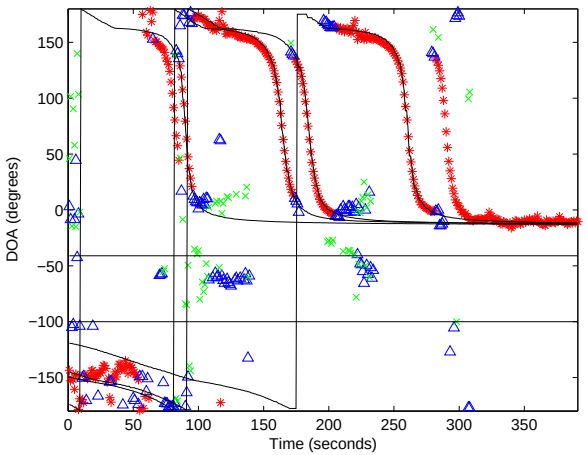

Beamspace Geometric Capon

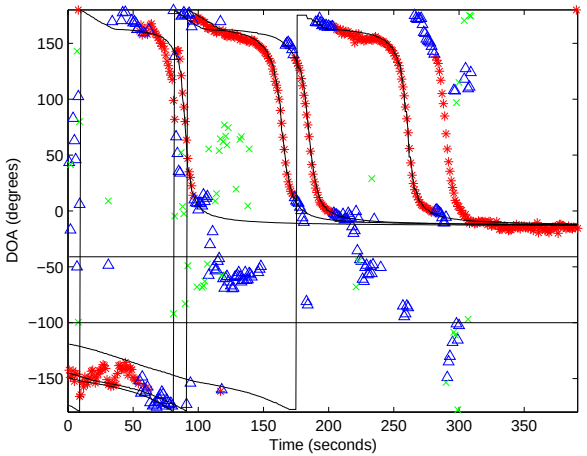

Standard Geometric Capon

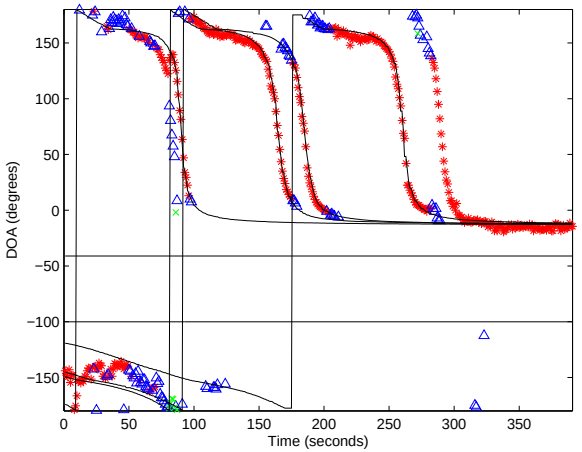

Geometric MUSIC

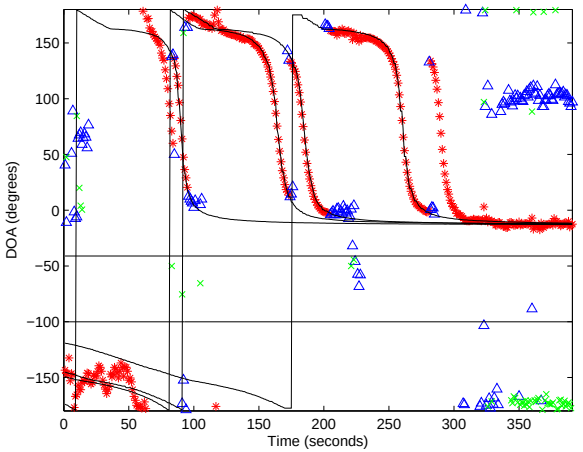

WSF

DOA estimation is the presence of high wind noise.

DOA Estimation Results - Distributed Run 3

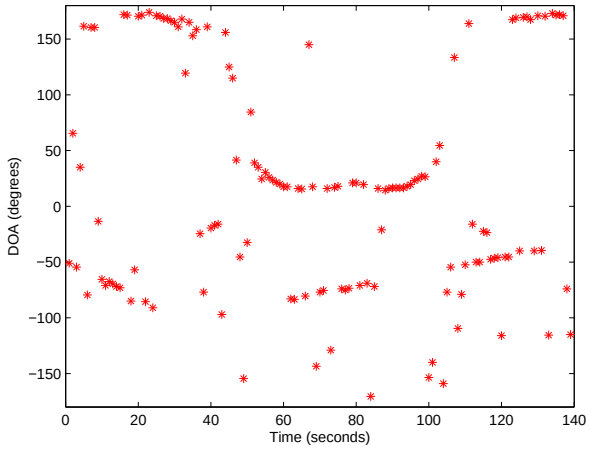

Arithmetic Capon

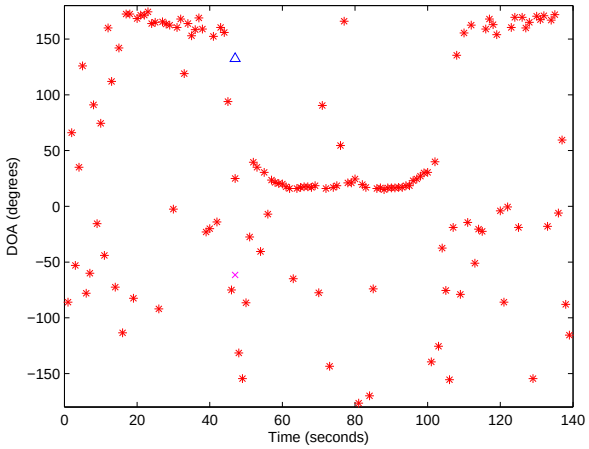

Geometric Capon

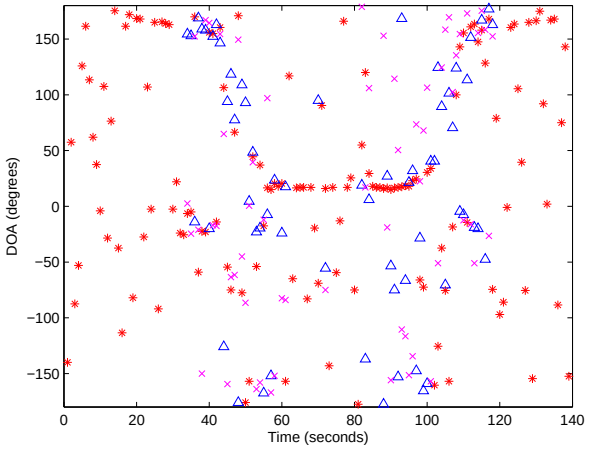

Harmonic Capon

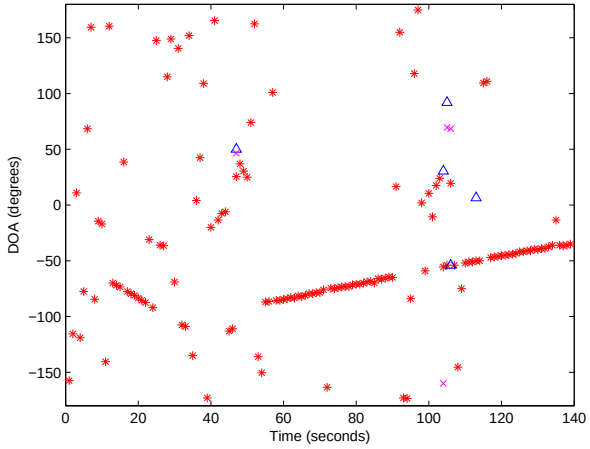

STCM

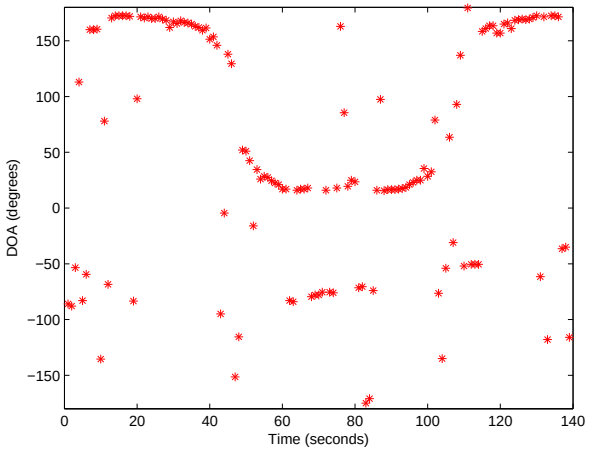

Geometric MUSIC

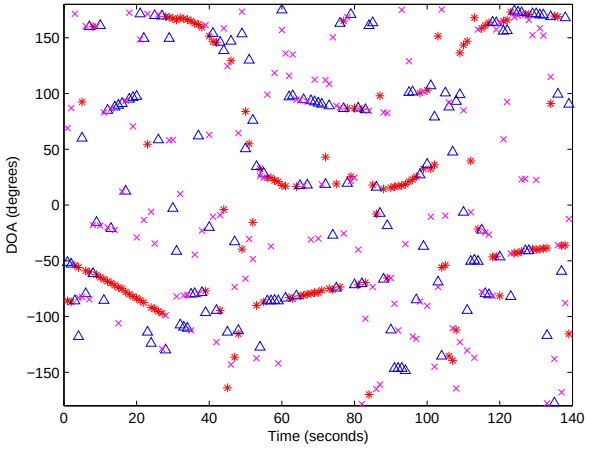

WSF

DOA estimation for a single extremely near-field source.

DOA Estimation Results - Distributed Run 3

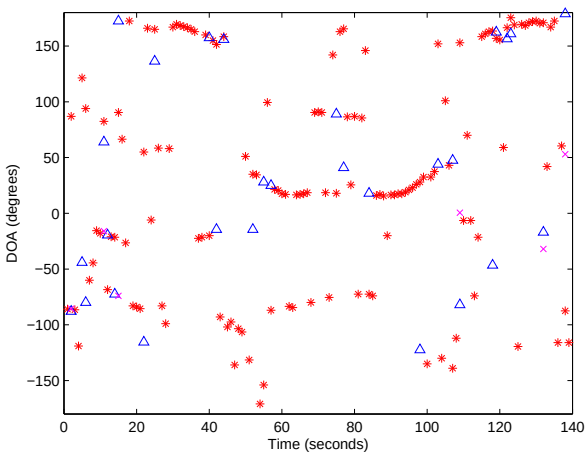

Beamspace Geometric Capon

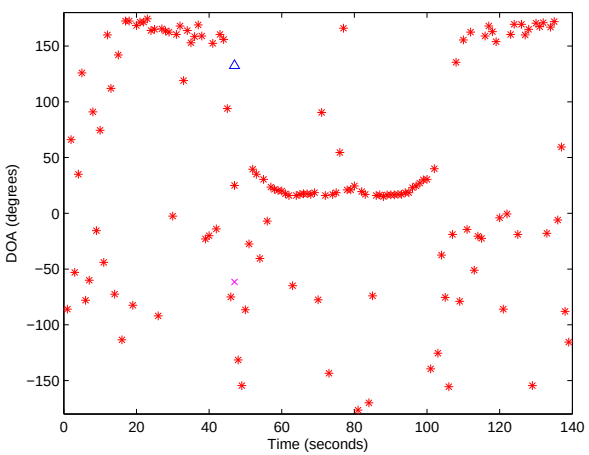

Standard Geometric Capon

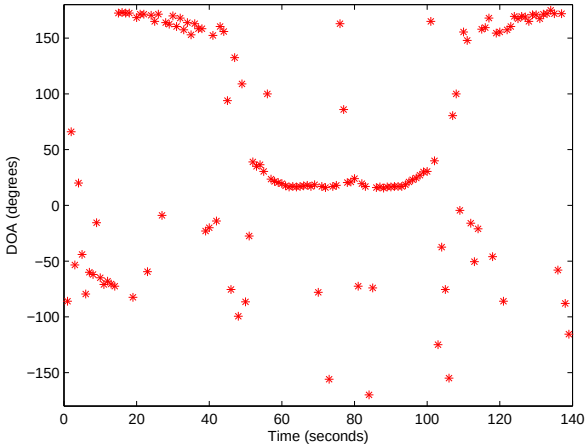

Robust Geometric Capon

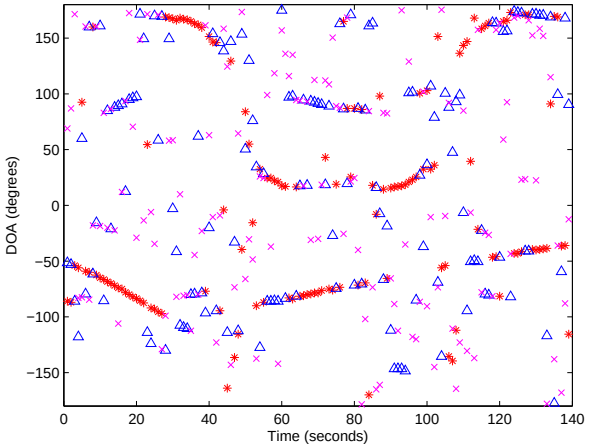

WSF

DOA estimation for a single extremely near-field source.

DOA Estimation Results - Distributed Run 3

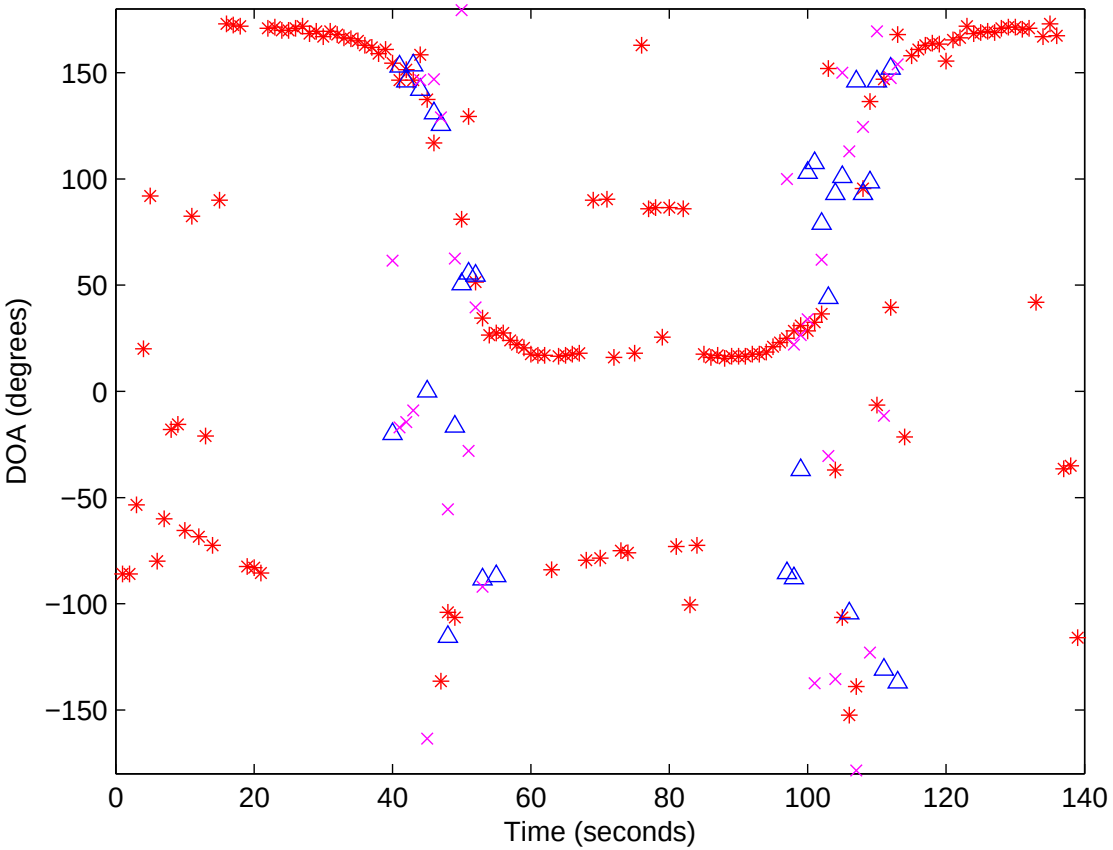

DOA Estimates using geometric robust Capon for Run 3 with estimated error of 10 (instead of 0.7).

Additional DOA Estimation Results - Distributed Run 4

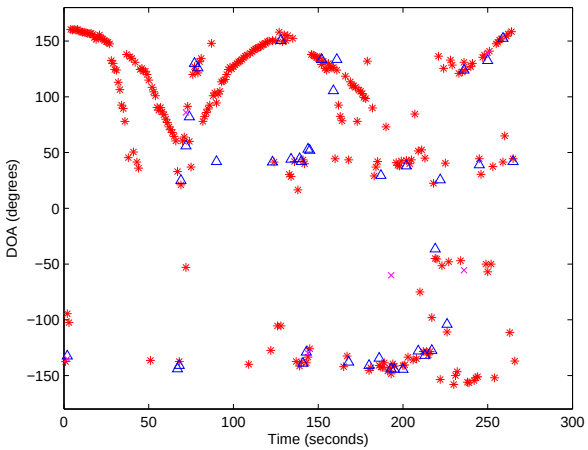

Beamspace Geometric Capon

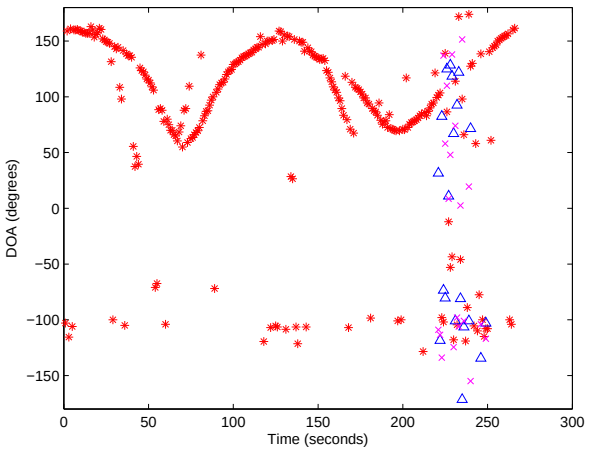

Standard Geometric Capon

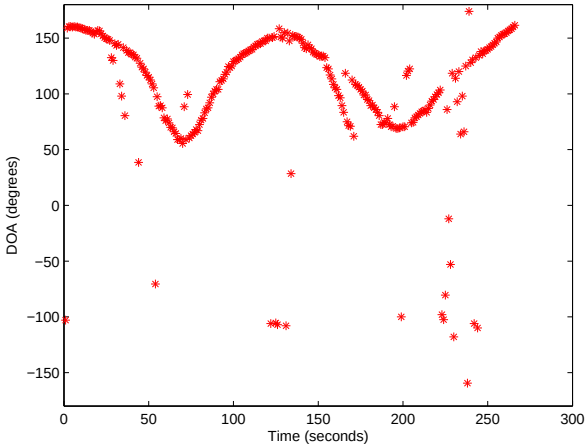

Robust Geometric Capon

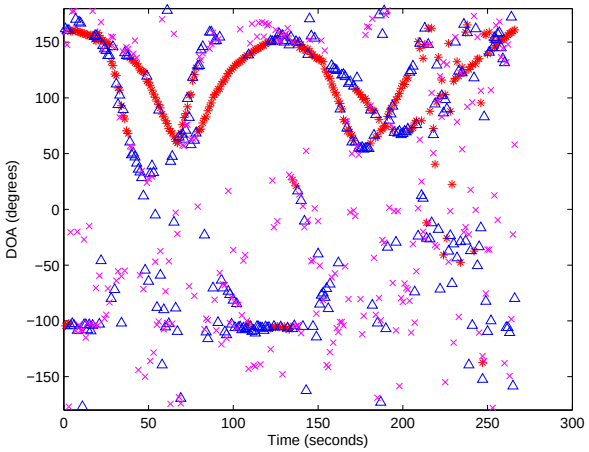

WSF

DOA Estimates on two source distributed array run 4.

Additional DOA Estimation Results - Distributed Run 5

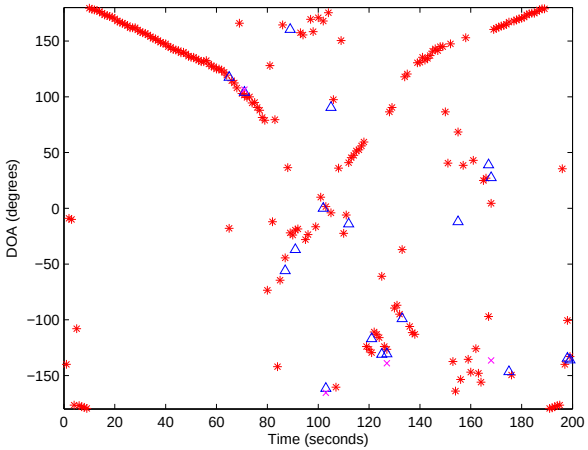

Beamspace Geometric Capon

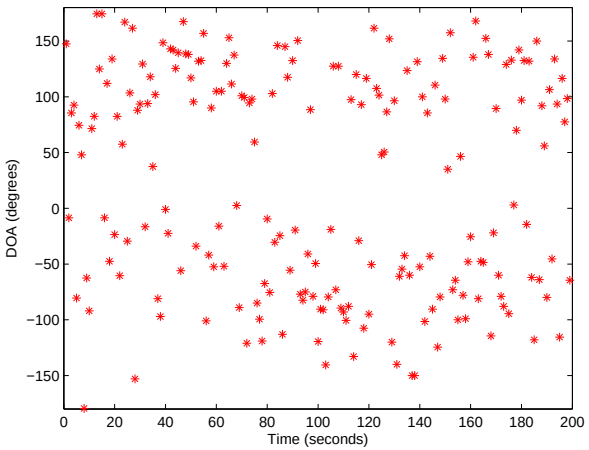

Standard Geometric Capon

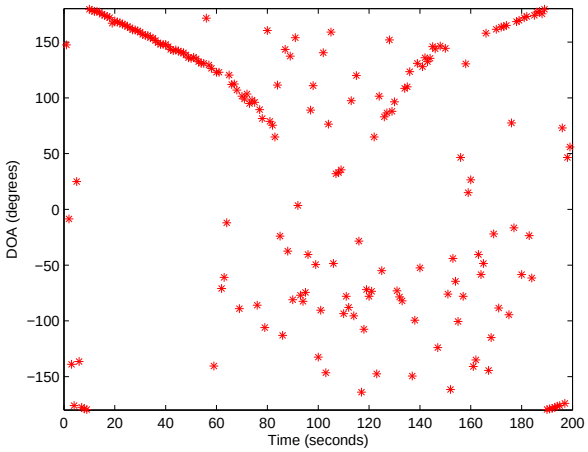

Robust Geometric Capon

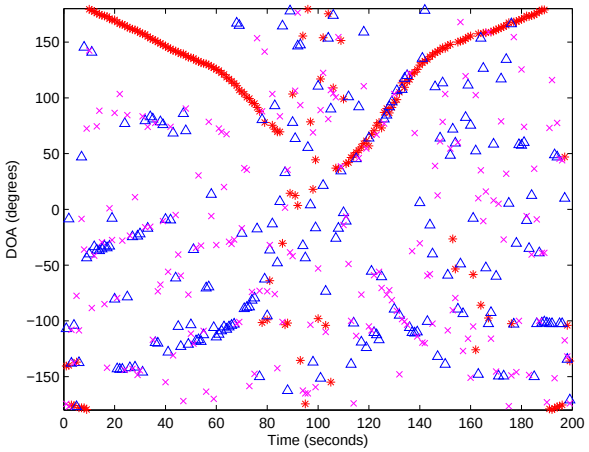

WSF

DOA Estimates for case with two sensor nodes that have missing data.